AN OPTIMAL SENSOR PLACEMENT DESIGN FRAMEWORK FOR STRUCTURAL HEALTH MONITORING USING BAYES RISK

Yichao Yang[1,*], Mayank Chadha[2,*], Zhen Hu[3] and Michael D. Todd[4,†]

[1,2,4]University of California San Diego, 9500 Gilman Drive, La Jolla CA 92093-0085, USA
[3]University of Michigan-Dearborn, Dearborn, MI 48128, USA
[1]yiy018@eng.ucsd.edu; [2]machadha@eng.ucsd.edu; [3]zhennhu@umich.edu; [4]mdtodd@eng.ucsd.edu

Key words: optimal sensor design; Bayes risk; Bayesian inference; uncertainty quantification; Bayesian optimization; surrogate modeling

Abstract. This paper presents a novel generalized framework for optimal sensor placement design for structural health monitoring (SHM) applications using Bayes risk as the objective function. Bayes risk considers the costs of consequences associated with making decisions and design selection (extrinsic cost) in the monitoring process, as well as intrinsic costs (e.g., sensor deployment and maintenance costs), which suggests that it is a natural choice for an SHM design objective function. The framework is intended to be sufficiently generalized to be applicable to any optimal sensor placement design used for SHM. To demonstrate the effectiveness and comprehensiveness of the proposed framework, it is applied to an example problem concerning the state detection of the boundary of a beam modeled by springs. We discuss in-depth the specific formulation of Bayes risk for this demonstration problem and detail multiple approaches to evaluate it. This paper addresses the challenges encountered in optimal sensor design problem due to the computationally expensive physics-based model, and it considers various uncertainties through the investigation and integration of Bayesian inference methods, uncertainty quantification, and optimization strategies. The effect of the initial design assumption and the technique used to approximate the Bayes risk on the final optimal sensor design is discussed.

1 Introduction

Structural health monitoring (SHM) may be generally defined as the process of making an assessment, based on appropriate analyses of in-situ measured data, about the current ability of a structural component or system to perform its intended design function(s) successfully. When coupled with future predictive capabilities, a successful SHM strategy may enable significant ownership cost reduction through maintenance optimization, performance maximization during operation, and unscheduled downtime minimization, and/or enable significant life safety advantage through catastrophic failure mitigation. Such an SHM strategy inevitably must, for a sufficiently well-defined application, include in-situ data acquisition, feature extraction from the acquired data, statistical modeling of the features, and subsequent hypothesis-based synthesis of the feature

*These authors contributed equally: Yichao Yang and Mayank Chadha
†Corresponding author

probabilistic models to make informed decisions about what to do with the structural component or system. Clearly, an important underlying enabler for an SHM strategy is the design of the sensor system, since data acquisition is the initiator of this multi-part paradigm [1, 2]. As no widely accepted sensing strategy in SHM has been adopted for use, this paper will propose and demonstrate the implementation of minimal Bayes risk as a natural target objective for SHM system design.

The application case that will be used in this paper is taken from the inland waterways infrastructure. The locks and dams that comprise the inland waterways infrastructure require an effective SHM system to prevent their unexpected failure and continuous monitoring in order to prevent huge economic losses [3, 4]. The United States Army Corps of Engineers (USACE) spends billions of dollars in maintaining and operating this infrastructure, where unscheduled shutdown of these assets and dewatering for inspection or repair is very costly [5, 6, 7, 8]. The need for SHM to help facilitate maintenance and operations appears strong, but highly constrained budgets suggest SHM system allocation efforts must be optimized to meet risk-based goals. Within the navigation lock systems, miter gates are one of the most common locking gates used; their most common failure mechanisms include long-term corrosion and loss of load-transferring contact in the quoin block (boundary related damage) [9]. As many of these structures have been operational for over 50 years, many are presently potentially operating in a higher-risk profile without engineers knowing their real structural capability [10]; current practice involves engineering elicitation via inspection, followed by lock closures if the inspection so warrants. Since this process is based on the varied experience and interpretation of field engineers, it bears high uncertainties and variability [11]. The use of SHM could potentially reduce those uncertainties, but the value of information obtained depends upon its design [12]. In general terms, the first step of the SHM system design is to decide what suitable sensors (e.g., strain-gauges, accelerators, etc.) provide measurements from which the extracted features are correlated to the type of damage or state to be inferred. The second step is then to obtain a sensor network design (e.g., number of sensors, location/placement, duty cycle, etc.) that provides the most valuable information at a minimal cost [13, 14, 15].

Numerous seminal contributions have been made in optimal sensor placement design for a wide class of SHM applications [16, 17, 18]. The overall goal of choosing the *best* sensor design is to let the monitoring system gather the most *effective* information from in-situ monitoring to detect the target state [19]. During the optimization process, an optimality criterion or an objective function is used to evaluate the effectiveness of the design. The best sensor design for a considered application, therefore, depends on the optimality criterion or objective function chosen. Thus, engineers from different fields may have different criteria for defining this to obtain the *best* design that leads to the most *effective* information use. In other words, the engineers look for the best objective function that is in line with the primary goal of the monitoring system, and it evaluates the value of that information in some way. Some classic such objective functions include the probability of detection (POD), and the probability of classification [20]. For instance, in the aviation sector, engineers maximize the probability of detection because the cost of life is assumed invaluable [21]. Papadimitriou et al. [22] have proposed sensor placement design by minimizing entropy focusing

on the applications of structural model updating. Similarly, Udwadia [23] and Basseville [24] have used the Fisher information matrix to maximize the parameter identification through SHM.

In many SHM systems used for large civil infrastructure such as the application area considered in this paper, the primary goal of the SHM system is to minimize the long-term monitoring and maintenance costs [5]. In this context, optimal sensor design is tied to the rate of incorrect decisions (e.g., the probability of false alarms for a binary decision case) and the costs/consequences associated with those wrong decisions. Flynn and Todd [25, 26] first introduced Bayesian experimental design [27] by minimizing expected loss or risk (also termed as Bayes risk) as a consequence of making the decision (choosing optimal design in their case). They demonstrated it in an ultrasonic guided wave sensor design problem. Bayes risk is proposed as a suitable choice of the objective function because it considers the costs of consequences associated with making decisions (parameterized by design selections in the monitoring process)–known as extrinsic costs, as well the cost of sensors system design, deployment, and maintenance–known as intrinsic costs. The optimal sensor design essentially demands arriving at the sensor network design that minimizes the expected losses as a consequence of making a decision, or equivalently, that minimizes the losses in an average sense (the idea adapted from Bayesian experiment design and Bayesian decision theory). Because the monitoring process is subject to many sources of noise and variability, structural state determination is inherently stochastic. Thus, the goal is to arrive at a sensor network design that considers all the uncertainties and the consequences of inferring the structural state using the data gathered by the design of interest. The prediction of the structural state bears a cost/risk. For example, if the predicted structural state is not the same as the true state (unknown), there will be an associated penalty in the form of planned or unplanned maintenance costs, operational availability losses, or even structural failure costs. The design that leads to the least expected loss/risk as a consequence of making structural state decisions is the optimal design. Since we are operating in an uncertain domain, arriving at an optimal design that minimizes Bayes risk is the best one can do. In this paper, Bayes risk will be used as an objective function in a strain-based measurement sensor optimization problem; however, we note that the framework proposed herein can also be applied to any SHM by formulating an appropriate form of Bayes risk constrained to that particular problem.

A common approach to function optimization includes iteratively evaluating the optimal value of the function locally guided by the steepest gradient descent. This approach has been used in machine-learning [28] and in developing an optimal sensor network [29]. Akbarzadeh [19] used a gradient descent algorithm in sensor optimization by deriving derivatives at each step, which requires less computational effort. However, in many problems, the exact analytical derivatives are not available. Agarwal [30] used the greedy algorithm to find a minimum number of sensors for covering a 2-dimensional space. The main shortcoming of the greedy algorithm is that it chooses the "current best" at each step so that it can easily converge to a local optimum instead of a global optimum. Heuristic algorithms are also widely used in the existing literature; for example, Jin [31] used a genetic algorithm to minimize the communication distance of sensors, while Yi et al. [32] utilized a genetic algorithm to obtain optimal sensor placement for a high-rise building

monitoring system. However, the main drawback of these optimization strategies is that they must run many samples, and hence are computationally expensive to arrive at the global optimal value of the objective function. In complex large-scale civil structures SHM applications, the sensor design space is potentially colossal. This coupled with the fact that obtaining and evaluating Bayes risk is computationally expensive and we do not have its derivatives, Bayesian optimization is the most suitable technique to apply. Bayesian optimization can optimize objective functions parameterized by high-dimensional design spaces with relatively low computational effort [33, 34, 35]. This paper details a general Bayesian optimization framework for obtaining the optimal sensor network design for SHM applications by using Bayes risk as the objective function. We address three implementation-based challenges: (1) Bayesian calibration of the discrete parameters defining the damage state; (2) the expensive evaluation of Bayes risk; and (3) the global optimization of an extremely high-dimensional design space informing Bayes risk.

After laying the theoretical foundation of Bayes risk and Bayesian optimization, we detail the general framework. We believe that the best possible way to demonstrate our sensor optimization framework is through an example that by itself doesn't pose tremendous uninformative challenges, is relatively simple to conceive, and has all the essential elements to utilize and showcase the optimization framework presented. To this end, we apply it to an example problem concerning the boundary condition detection state of a beam structure. This example was considered because it covers a broader spectrum of detection and inference-type problems that are common in SHM. One instance of a resembling but slightly different problem is that of contact loss detection between the quoin blocks of the miter gate. Moreover, the demonstration example is sufficiently complex to highlight the sensor optimization framework and the associated challenges while not inducing computational complexities and costs associated with more complex structural scenarios.

The rest of the paper is arranged as follows. Section 2 briefs the concepts of the Bayes risk functional and explains the four steps of the general sensor optimization framework. Section 3 describes the demonstration problem and details the associated Bayes risk functional, followed by Section 4 that investigates three different approaches to evaluate the Bayes risk. Section 5 discusses the optimal sensor placement design using Bayesian optimization in detail and presents the algorithm used. After a general discussion on Bayesian optimization, the remaining part of Section 5 discusses the effect of the initial design assumption and the approaches used to evaluate the Bayes risk on the final optimal sensor design for the demonstration problem. We present three methods to evaluate the Bayes risk functional: a sampling-based method, mean-value approximation, and univariate dimensional reduction with Gauss-Hermite quadrature. The sampling-based method yields the most accurate Bayes risk if large sample size is considered. Consequently, the sampling-based method suffers from a high computational cost. This drawback makes the sampling-based method unsuitable for sensor placement optimization. Secondly, as is the inherent case with any Monte-Carlo based approach, the values of Bayes risk obtained from the sampling-based technique change as a different set of samples are chosen. The other two methods overcome these challenges and disadvantages. However, the mean-value approximation of the Bayes risk does not yield accurate

values. The univariate dimensional reduction with Gauss-Hermite quadrature is fairly accurate and has acceptable computational speed. Therefore, we use this third approach to evaluate Bayes risk, and then Bayesian optimization follows. Finally, Section 6 concludes the paper and lists ongoing research directions.

2 Bayes risk and general optimization framework

We first present some preliminary definitions and notations. The real number space is represented by $\mathbb{R}$. A random variable X is a real-valued function defined on a discrete or a continuous sample space S_X and the measurement space Ω_X, such that $X : S_X \longrightarrow \Omega_X \subset \mathbb{R}$. Let x represent the realization of the random variable X, such that $x \in \Omega_X$. The probability density function and the cumulative density function is represented by $f_X(x \in \Omega_X)$ and $F_X(x \in \Omega_X)$. The expected value of a function $g(x)$ is denoted by $E_X[g(x)]$. Lastly, a random variable X following Gaussian distribution, with the mean μ_x and standard deviation σ_x is denoted by:

$$\begin{aligned} f_X(x) &= \frac{1}{\sigma_x}\phi\left(\frac{x-\mu_x}{\sigma_x}\right); \\ F_X(x) &= \Phi\left(\frac{x-\mu_x}{\sigma_x}\right); \\ X &\sim N(\mu_x, \sigma_x). \end{aligned} \tag{1}$$

2.1 Bayes risk for decision-making

Generally speaking, for a problem concerning Bayesian decision-making, the goal is to arrive at a decision that minimizes the expected risk (also referred to as Bayes risk in this paper) or expected loss. The idea is that we have information about the system in the form of observable measured data. The goal is to learn the behavior of the system from the data (called training) and then use the learned model to predict the *outcome*. Primarily, the outcomes can be categorized by detection, classification, and regression. For instance, detecting if the structure is *damaged* or *not damaged* given the measured strain gauge data is an example of detection; grouping the *raw grades* of the class into the *letter grades* is an example of classification; developing a *digital twin/surrogate* of a non-linear system is an example of regression. The goal is to make a decision that minimizes the expected loss or risk that arises as a consequence of making a decision (every action/decision has a consequence). Therefore, the optimality criterion used in this paper is the expected loss/risk, which is also referred to as Bayes risk functional and is a problem-dependent quantity. The strong similarity of Bayes risk with the action functional in variational structural mechanics is not surprising.

We focus on the classification type problem of which detection is a special case. Let Ω_X represents the measurement space, Ω_Y represents the true state (or outcome) space with M classes (for detection as defined above, $M = 2$), such that the feature/measurement/observable is $x \in \Omega_X$,

true outcome (or decision) is $y \in \Omega_Y = \{y_0,\ y_1, ...,\ y_{(M-1)}\}$, and the predicted outcome (or decision) is $g(x) \in \Omega_G = \{g_0,\ g_1, ...,\ g_{(M-1)}\}$, where $i = \{0, 1, ..., (M-1)\}$. Let X, Y, and G represent the random variables corresponding to the uncertain measurement space, the true outcome, and the predicted outcome respectively. Note that $\Omega_G \equiv \Omega_Y$, and the two representations of outcome space is to distinguish between the *true* (but unknown) and the *predicted* states. In fact, $g(x)$ represents the trained model. For instance, in the case of a simple detection problem, y_0 denotes a true damaged state; and g_0 is a prediction of a damaged state. Bayes risk is designed such that it minimizes the effects of incorrect decisions. This is done by incorporating a loss function $L(g(x), y) : \Omega_G \times \Omega_Y \longrightarrow \mathbb{R}$. It defines the consequence-cost of deciding the outcome to be $g(x)$ when y is the true outcome. Since our goal is to minimize losses incurred as a consequence of making a data-informed decision that could be possibly incorrect, the Bayes risk (objective functional) is defined as the expected loss, averaged over all possible (noisy) measurements and the true state y_i. Since the goal in this section is to estimate the state $g(x)$ when the true state is y using the measurement x, the Bayes risk Ψ_{state} is a function of the predicted outcome/state $g(x)$ which in turn is a function of newly acquired data $x \in \Omega_X$. The Bayes risk is then defined as:

$$\begin{aligned}\Psi_{\text{state}}\left(g(x)\right) = E_{XY}\left[L(g(x), y)\right] &= \sum_{i=0}^{M-1} \int_{\Omega_X} f_{XY}(x, y_i) L(g(x), y_i)\, \mathrm{d}x \\ &= \sum_{i=0}^{M-1} \int_{\Omega_X} L(g(x), y_i) P_{X|Y}(x|y_i) P_Y(y_i)\, \mathrm{d}x.\end{aligned} \tag{2}$$

Bayes risk can also be written in terms of *conditional risk* $R_{\text{state}}\left(g(x)\right)$, conditioned on measurement x, as:

$$\Psi_{\text{state}}\left(g(x)\right) = E_X\left[R_{\text{state}}\left(g(x)\right)\right] = \int_{\Omega_X} f_X(x) R_{\text{state}}\left(g(x)\right)\ \mathrm{d}x, \text{ where,} \tag{3a}$$

$$R_{\text{state}}\left(g(x)\right) = \sum_{i=0}^{M-1} L(g(x), y_i) f_{Y|X}(y_i|x). \tag{3b}$$

The conditional risk is defined as the expected loss averaged over all possible true states and considering (or conditioned on) fixed measurement x. The optimal decision is the one that minimizes the expected loss, or,

$$\mathfrak{g}(x) = \arg\min_{g(x)} R_{\text{state}}(g(x)) \in \Omega_G. \tag{4}$$

The Bayes risk $\Psi_{\text{state}}\left(g(x)\right)$ defined in this section is an objective functional that is used to optimally predict the most likely state $g(x)$ given the measurement x (hence the subscript *state* in Ψ_{state} and R_{state}). However, among possible choices of an SHM system design, every design will predict a unique state for a given set of measurements (obtained by (4)). Inversely, the predicted outcome is dependent on the sensor design. In the next section, we consider the problem of design selection that would warrant a different Bayes risk functional. The goal is to pick the design that leads to the

least erroneous state estimation (the optimality criterion is defined in the next section). Unlike the problem of state-estimation, where Bayes risk was a function of the estimated state $g(x)$, the Bayes risk for the design selection, represented by $\Psi_{\text{design}}(e)$, will be a function of design e.

2.2 Bayes risk for design selection and optimal sensing framework

The primary goal of this paper is to arrive at an optimal sensing design, and Bayes risk can accommodate this notion. Let Ω_E represent the design/experiment space, such that $e \in \Omega_E$ represents a design realization. Every design e yields different measurement data $x_e \in \Omega_{X_e}$, and corresponding likelihoods $f_{X_e|Y}(x_e|y)$. Here, Ω_{X_e} represents the measurement space for the design e, and X_e denotes the corresponding random variable. Let $\mathfrak{g}(x_e; e)$ represents the optimally estimated state obtained using Eq. (4) for the measurement x_e corresponding to the design $e \in \Omega_E$. Therefore, the decision $\mathfrak{g}(x_e; e)$ is also design-dependent. In other words, we now care about choosing the design with the least error/deviation in the decision $\mathfrak{g}(x_e; e)$ relative to the true value y. Equation (4) can be used to arrive at the optimal state $\mathfrak{g}(x_e; e)$ for a given design e; or equivalently, for each design e, a threshold (or a classifier) can be established using Eq. (4) in the measurement space Ω_{X_e} that helps classify each realization of measurement x_e into the optimal state $\mathfrak{g}(x_e; e)$. Therefore, Eq. (4) establishes a mapping between the continuous measurement parameter x_e and the decision (discrete in case of detection problem) $\mathfrak{g}(x_e; e)$. This allows us to write the Bayes risk for each design e focusing on minimizing the deviation of the predicted outcome $\mathfrak{g}(x_e; e)$ relative to the true outcome y as:

$$\Psi_{\text{design}}(e) = E_{GY}\left[L(\mathfrak{g}(x_e; e), y)\right] = \sum_{i,j=0}^{M-1} L(g_i, y_j) f_{G|Y}(\mathfrak{g}(x_e; e) = g_i|y_j) f_Y(y_j), \text{ where,} \tag{5a}$$

$$f_{G|Y}\left(\mathfrak{g}(x_e; e)|y\right) = \int_{\Omega_{X_e}} f_{G|X_e}\left(\mathfrak{g}(x_e; e)|x_e\right) f_{X_e|Y}(x_e|y)\, \mathrm{d}x_e. \tag{5b}$$

For a design e, the true state y, and the observed measurement x_e, the estimated state $\mathfrak{g}(x_e; e)$ is one of the states in the set Ω_G. Equivalently, for a design e, the true state y, and the measurement x_e, every state $g_i \in \Omega_G$ has a likelihood probability of $f_{G|Y}(\mathfrak{g}(x_e; e) = g_i|y)$ to be selected as the optimal estimated state $\mathfrak{g}(x_e; e)$. The Bayes risk functional $\Psi_{\text{design}}(e)$ defined in Eq. (5a) calculates the expected value of loss (or risk) considering all the possibilities of the estimated states $\mathfrak{g}(x_e; e) \in \Omega_G$ and considering all the possible true states $y \in \Omega_Y$. Minimizing this function yields a design that leads to the best prediction of the state. We will adapt the Bayes risk defined in Eq. (5a) focusing on a detection-type problems common in SHM. The following paragraphs detail the generalized step-by-step procedure for the proposed optimal sensor framework.

Step 1: Problem description

The first step involves a well-defined problem description. We need to decide our decision and the true space (Ω_G, Ω_Y), or what needs to be detected, and what is its true condition/state, respectively. Both, the decision and the true space refer to the state of the structure defined accordingly. A discrete decision space in SHM answers the question "Is a structure critically damaged or not?", e.g., whether a bolted assembly is at design torque or not; a continuous decision space, such as where regression may be utilized, might be to infer crack length. In this paper, we focus on discrete decision spaces, but at the same time note that the framework can easily be extended to the continuous case. In theory, that would essentially replace the summation over the decision space in Eq. (5a) by an integral. In practice, the continuous decision space can be discretized by identifying the mutually exclusive and exhaustive subsets with a decision state. For instance, a corroded surface area $< 10\%$ of a bridge girder might be classified as *not damaged*, $10\% - 30\%$ can be identified as *moderately damaged*, and $> 30\%$ can be considered as *severely damaged*. Secondly, we need to define the measurement of the observable quantity using which the structural state is inferred. The features used to infer the structural state can be extracted from the measured quantity, although the measured data itself can be the feature. The measurement space Ω_{X_e} essentially is the space from which the decision is directly inferred; therefore, in current content, the measurement space is the feature space. Once we know what needs to be measured (for example, strain values), the design space Ω_E follows (e.g., all the possible arrangements of a strain gauge network). Therefore, the problem description consists of defining the decision space, the true state space, the measurement (or feature) space, and the design space.

Step 2: Definition of the design dependent Bayes risk functional

For a simple classification problem, Eq. (5) represents the Bayes risk functional. However, as the complexity of the problem evolves, suitable adjustments to the Bayes risk should be made. For instance, in our demonstration problem described in detail later, where we are focusing on the problem of multiple load path changes through boundary connections, the space of collective true states of the springs (denoted by Ω_A) becomes important. Second, in the case of collective decision-making problems, some decisions are more preferred or weighed than others. To incorporate such situations, we can assign weights to each of these decisions. Third, unlike the Bayes risk expression in Eq. (5) that incorporates the cost of making a decision or extrinsic cost only, the intrinsic costs (like the sensor deployment and maintenance costs) must be included in SHM applications. All these considerations lead to Bayes risk $\Psi_{\text{design}}(e)$ to bear a form defined in Eq. (9), with the extrinsic cost defined in Eq. (10) of Section 3.2.

Step 3: Evaluation of the design-dependent Bayes risk functional

For a Bayes risk of a simple classification or detection type problems represented in Eq. (5a), the first challenge is to evaluate the three probabilities present in Eq. (5): $f_Y(y_j)$, $f_{X_e|Y}(x_e|y)$, and

$f_{G|X_e}(\mathfrak{g}(x_e;e)|x_e)$. The quantity $f_Y(y_j)$ represents the prior probability of the true state, and in absence of any information can be assumed as 0.5 for a detection type problem. The likelihood $f_{X_e|Y}(x_e|y)$ is obtained using either a physics-based model or a digital twin. The posterior of the decision given the measurement $f_{G|X_e}(\mathfrak{g}(x_e;e)|x_e)$ is more involved to evaluate. For a binary detection problem it can be written using the law of total probability as:

$$f_{G|X_e}(g_i|x_e) = \sum_{j=1}^{2} f_{G|Y}(g_i|y_j) f_{Y|X_e}(y_j|x_e). \tag{6}$$

The probability of making a decision given the true state $f_{G|Y}(g_i|y_j)$ depends on the detection threshold evaluated for each design case using Eq. (4). The quantity $f_{Y|X_e}(y_j|x_e)$ is anti-causal and can be evaluated using Bayes theorem as:

$$f_{Y|X_e}(y_j|x_e) = \frac{f_{X_e|Y}(x_e|y_j) f_Y(y_j)}{f_{X_e}(x_e)}. \tag{7}$$

The second difficulty in obtaining Bayes risk is to evaluate the integral in Eq. (5b). To approximate the integral, we first change the variable of the integral from the measurement space to the uncertain input space. For instance, in our demonstration problem, the load, its location, and the noise in the strain values are uncertain, causing randomness in the strain measurement. We realize that a unique value of the load, its location, and the noise in the strain gauge give a unique realization of the strain measurement. This allows us to change the variables of integration as defined in Eq. (17). The integral can then be numerically approximated. We discuss three different approaches to evaluate the integral in Section 4.4.

Step 4: Obtaining the optimal sensor design using Bayesian optimization

Once the problem is well defined (step 1) and the associated Bayes risk is obtainable (steps 2-3), the question that we intend to answer for optimal sensor design is: "*Given* Ω_G, Ω_Y, Ω_{X_e}, *and* Ω_E, *and given an assumed initial design* e_0, *what is the design* $e^* \in \Omega_E$ *that minimizes the Bayes risk* $\Psi_{\text{design}}(e)$?"

We very briefly detail the sensor optimization algorithm, which will be explained in great depth in Section 5. We start with an initial design e_0 consisting of N_0 number of sensors. To obtain the optimal design e_1 with (N_0+1) sensors, we search the entire design space for the $(N_0+1)^{\text{th}}$ sensor location. The $(N_0+1)^{\text{th}}$ sensor location that maximizes the acquisition function constitutes the next additional sensor. In this paper, we use *expected improvement* [36, 37] as the acquisition function. Similarly, we repeat the optimization process to arrive at the optimal design $e_{n_{\text{as}}}$ consisting of $N_0 + n_{\text{as}}$ sensors (or n_{as} number of additional sensors relatively to the initially assumed design e_0). Finally, we pick $e^* = \arg\min_{e_{n_{\text{as}}}} \Psi_{\text{design}}(e_{n_{\text{as}}})$ as the most optimal design, where $\Psi_{\text{design}}(e_{n_{\text{as}}})$ represents the Bayes risk associated with the design $e_{n_{\text{as}}}$. Figure 1 illustrates the pipeline of the proposed Bayesian optimization framework. Section 3 deals with the description of a demonstration

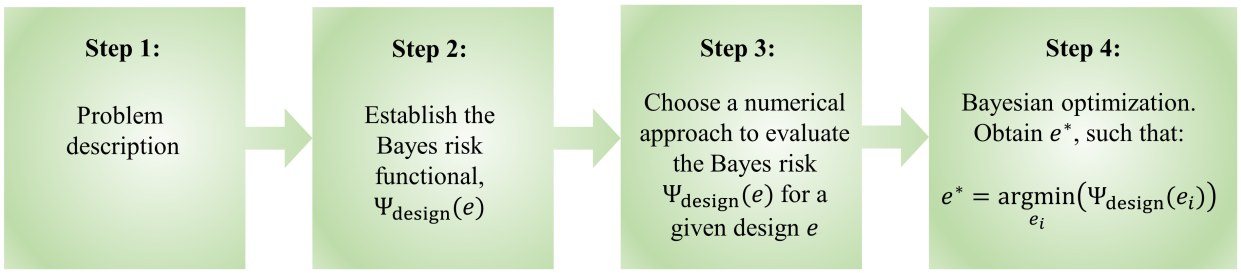

Figure 1: Bayesian optimization framework for optimal sensor network design

problem and derives the associated Bayes risk (steps 1 and 2). Section 4 discusses the approaches to evaluate the Bayes risk pertaining to the demonstration problem (step 3). Finally, Section 5 details the Bayesian optimization algorithm for optimal sensor placement 1 for general detection-type problems and discusses the results concerning the demonstration problem.

3 Demonstration problem description and the associated Bayes risk

As we mentioned in the introduction, our primary motivation for choosing the following example problem as a case study to demonstrate this framework is that it resembles in behavioral characteristics a typical detection-type problem in SHM that has a discrete decision space: the loss of contact in the quoin block of a miter gate. As discussed in Section 2.2, even the continuous decision space can be reasonably broken down into a rather more convenient discrete decision space. Hence, the presented framework is also suitable for problems involving crack propagation, corrosion, weld defect growth, etc. To demonstrate the framework, we consider a beam modeled by 2D shell elements and focus on detecting the state of the boundary modeled using connecting springs. This problem is complicated enough to highlight the Bayesian optimization framework for sensor placement and undemanding enough to implement our algorithms with a lower computational cost. The figure below shows similar types of problems in SHM where the presented sensor-design framework can be extended (although each specific problem would require it's own carefully considered Bayes risk functional).

3.1 Demonstration problem description

The demonstration problem consists of a cantilever beam supported by a roller on the left end and a free boundary on the right end. The Young's modulus of the beam is $2.1 \times 10^9 Nm^{-2}$. There exist 11 wall-to-beam springs with the stiffness $10^7 Nm^{-1}$ connected to the left side of the 2D shell

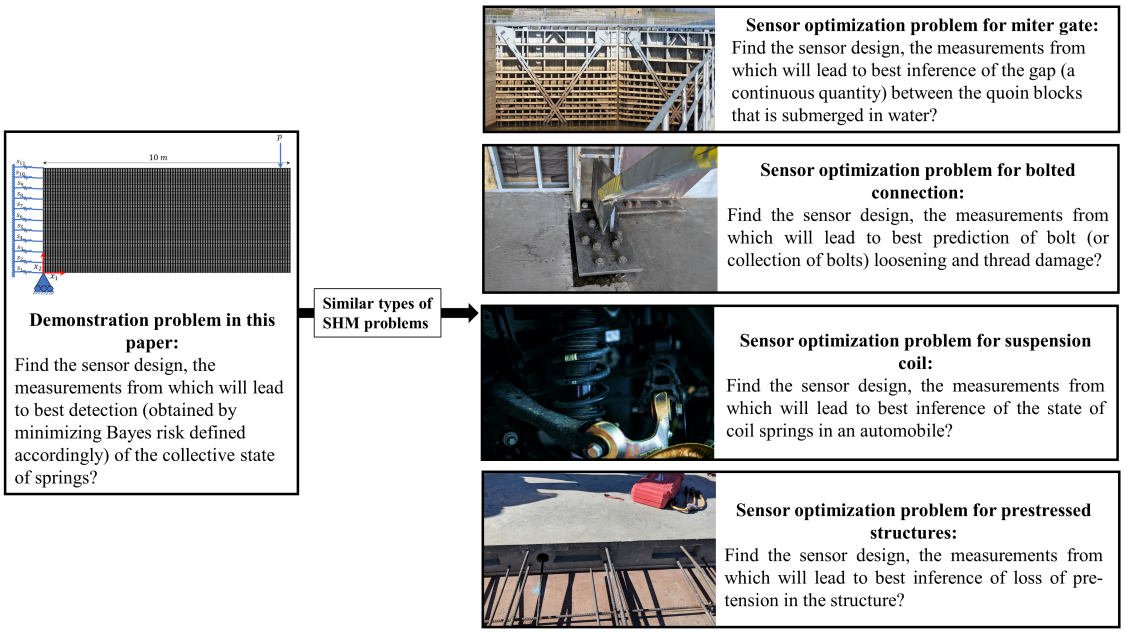

Figure 2: Design optimization problems in SHM similar to the demonstration example presented in this paper

element providing structural stability as shown in Fig. 3. The finite element model for the beam was build in OpenSees [38] with quadrilateral meshing. The entire beam was meshed finely to 22500 elements to capture accurate strain responses, particularly at the left edge of the beam, where the springs are attached. The horizontal axial strain of the element is considered to be the strain gauge measurement. Therefore, there are 22500 possible strain gauges (with horizontal orientation). In the general case, the strain gauge may be discrete or continuous and can have any orientation [39].

Our problem statement is as follows: we aim to arrive at the best possible *sensor placement design* $e \in \Omega_E$, where Ω_E is the design space, such that the existence of the springs on the left of the beam can be most optimally predicted ("detected"), given that the magnitude of the load p and its location $p_{\text{loc}} \in [0, 10]$ are uncertain. We also assume that the strain gauge readings are noisy. By *sensor placement design*, we mean the arrangement of the strain gauges (including the number used and their locations). To simplify the problem further, we fix the top six springs. Hence, we need not predict their existence. Our goal is, therefore, to predict the existence of the remaining five springs s_1, s_2, s_3, s_4, and s_5.

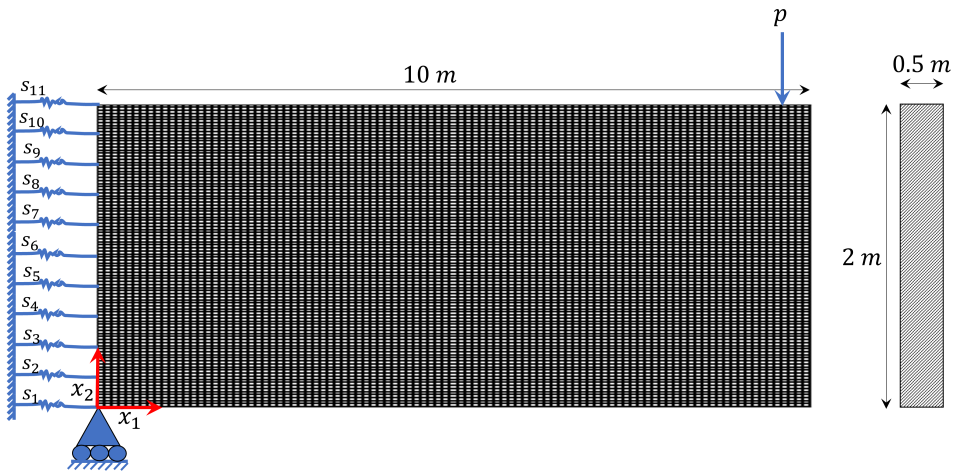

Figure 3: Schematic diagram of the 2D beam modeled by 2D shell elements

3.2 Bayes risk for the optimal sensor placement

As discussed before, for each spring, our *predicted decision space* Ω_G and the *true outcome space* Ω_Y consist of two possible outcomes, such that $\Omega_G = \{g_0,\ g_1\}$ and $\Omega_Y = \{y_0,\ y_1\}$, where

$$\begin{aligned} g_0 &: \text{ Prediction is that the spring exists;} \\ g_1 &: \text{ Prediction is that the spring does not exists;} \\ y_0 &: \text{ True state is that the spring exists;} \\ y_1 &: \text{ True state is that the spring does not exists.} \end{aligned} \tag{8}$$

Recall that we have 5 critical springs s_n, with $n \in \{1, 2, 3, 4, 5\}$. For n^{th} spring, we denote the predicted state by $g_i|_{n^{\text{th}}\text{spring}} = g_{ni}$, and the true state by $y_j|_{n^{\text{th}}\text{spring}} = y_{nj}$, with $i, j \in \{0, 1\}$, such that $g_{ni} \in \Omega_G$ and $y_{nj} \in \Omega_Y$. Since there are five springs, with each of them existing in the either of two possible states $\{y_0, y_1\}$, there are 2^5 possibles states of the springs collectively. We define the *collective true state* of the five springs by a set of vectors Ω_A, such that $A_k = [\bar{y}_1, \bar{y}_2, \bar{y}_3, \bar{y}_4, \bar{y}_5] \in \Omega_A$ and $\bar{y}_n \in \{y_{n0}, y_{n1}\} = \Omega_Y$, with $k \in \{1, 2, 3, ..., 2^5\}$, and $f_A(A_k) = 2^{-5}\ ,\forall\ k$. Similarly, we define the *collective prediction state* of the five springs by a set of vectors Ω_S, such that $S_k = [\bar{g}_1, \bar{g}_2, \bar{g}_3, \bar{g}_4, \bar{g}_5] \in \Omega_S$ and $\bar{g}_n \in \{g_{n0}, g_{n1}\} = \Omega_G$, with $k \in \{1, 2, 3, ..., 2^5\}$. We define A and S as the random variables corresponding to the space Ω_A and Ω_S respectively, such that, A_k and S_k represents the realizations of A and S respectively.

For the considered sensor placement design e, the Bayes risk specific to this problem consists of *intrinsic* and *extrinsic* costs. The intrinsic cost $\Psi_{\text{design-in}}(e)$ includes the expenses associated with the sensor installation and maintenance. On the other hand, the extrinsic cost $\Psi_{\text{design-ex}}(e)$ accounts for the cost of making a decision and the design selection. It resembles the form of Eq. (5).

Therefore, the total Bayes risk is defined as:

$$\Psi_{\text{design}}(e) = \Psi_{\text{design-in}}(e) + \Psi_{\text{design-ex}}(e). \tag{9}$$

We now focus on constructing the extrinsic cost $\Psi_{\text{ex-design}}(e)$. We denote the cost $L\left(g_{ni}, A_k\right) : \Omega_G \times \Omega_A \longrightarrow \mathbb{R}$, defining the regret of making the decision g_i for the strain gauge n, when the true *collective state* is A_k. We further define the cost function: $C_{nij} = L\left(g_{ni}, A_k(n) = y_{nj}\right)$, and assume that it is independent of the selected design e. For the fixed spring n, the cost $C_{nij} = C_{ij}$ is defined as:

		True State	
		y_0	y_1
Predicted State	g_0	C_{00}	C_{01}
	g_1	C_{10}	C_{11}

Table 1: Cost function

The cost values C_{ij} assign penalty/losses to each predicted state g_i when the true state is y_j. Consider the case where the spring exists in reality, i.e. the state y_0. If the prediction is correct, i.e. g_0, there is no loss since no action is warranted, or $C_{00} = 0$. On the contrary, if the prediction is g_1 (spring not existing), then the engineers would decide to perform unnecessary inspection and service leading to a loss of C_{10}. However, as a consequence of this incorrect decision, there would be no major failure since the spring exists in reality. Similarly, consider the case where the spring does not exist, represented by y_1 (the boundary is actually damaged). If we estimate (from strain gauge data) that spring does not exist (correct decision), then there will be cost (denoted by C_{11}) incurred to inspect and repair the spring (or the boundary). However, if the spring is predicted to exist, when it is non-existent (incorrect decision), it can lead to the most expensive mistake since the structure can potentially fail if appropriate actions are not taken. This leads to the maximum cost of C_{01}. For simplicity, we assume $C_{01} = 200$ dollars and assume other costs to be fraction of C_{01}, such that $C_{10} = 0.1C_{01}$ and $C_{11} = 0.25C_{01}$. Individual costs C_{ij} are defined in Table 2.

Cost	**Definition**	**Breakdown**	**Assumed Dollars**
C_{00}	True positive cost	Zero cost, as no action is needed	0
C_{10}	False positive cost	Cost due to service and inspection	20
C_{01}	False negative cost	Cost due to service, failure, and replacement	200
C_{11}	True negative cost	Cost due to service and repair	50

Table 2: Assumed cost function values

In cases of problems involving multiple decisions, there may be instances where the consequences of making some decisions are more important or weighed for some cases than the others (like some springs being more important than the others). To incorporate these kind of situations, we assume that the top two springs (s_4, s_5) are more important than the bottom three (s_1, s_2, s_3). We

incorporate this assumption by assigning weights to each of these springs as $w = [1,\ 1,\ 1,\ 1.5,\ 1.5]$. Our goal is to define the extrinsic Bayes risk functional, considering the importance of the consequence of decisions associated with each spring, as a quantity that minimizes itself with the most optimal sensor arrangement e. Along the similar lines of Eq. (5), the extrinsic Bayes Risk is defined as:

$$\Psi_{\text{design-ex}}(e) = \sum_{n=1}^{5} w_n E_{GA}\left(L\left(g_{ni}, A_k\right)\right) = \sum_{n=1}^{5} w_n \sum_{k=1}^{32}\sum_{i=0}^{1} L\left(g_{ni}, A_k\right) f_{G|A}(g_{ni}|A_k) f_A(A_k). \quad (10)$$

In the equation above, $f_A(A_k) = 2^{-5}$ is the prior probability of the collective state of springs being A_k. Secondly, $x_e \in \Omega_{X_e}$ represents the measured/observed data. For instance, x_e can be strain measurements for any design e. For the n^{th} spring, the quantity $f_{G|A}(g_{ni}|A_k)$ represents the probability of predicting the state g_i for the spring n, when the true collective state is A_k. This is a difficult bit to evaluate, and like Eq. (5b) can be broken down into more manageable pieces:

$$f_{G|A}(g_{ni}|A_k) = \int_{\Omega_{X_e}} f_{G|X_e}(g_{ni}|x_e).f_{X_e|A}(x_e|A_k)\,\mathrm{d}x_e. \quad (11)$$

The likelihood $f_{G|X_e}(g_{ni}|x_e)$ depicts our belief of deciding the state of the spring n to be g_i for a given measurement $x_e \in \Omega_{X_e}$. We obtain the likelihood using Bayesian inference (detailed in next section).

4 Evaluating Bayes risk for a fixed design

To perform Bayes optimization that yields the most optimal sensor placement design, we will have to start with a design that evolves/improves with every iteration of the optimization process. At every iteration, for a suggested design e, we need to obtain the Bayes risk defined in Eq. (10). Therefore, in this Section, we detail on calculating the Bayes risk for a design e consisting of 30 sensors, the arrangement of which was obtained using *Latin Hypercubic Sampling* (LHS) technique [40]. The first step of the process is to evaluate the likelihood of making a decision given the measurement, $f_{G|X_e}(g_{ni}|x_e)$.

4.1 Analytical formulation to obtain the likelihood

The goal is to obtain $f_{G|X_e}(g_{ni}|x_e)$. Recall that $S_k \in \Omega_S$ defines the collective prediction state of the springs. We can therefore write:

$$f_{G|X_e}(g_{ni}|x_e) = \sum_{k=1}^{32} f_{G|S}(g_{ni}|S_k).f_{S|X_e}(S_k|x_e). \quad (12)$$

We note that:

$$f_{G|S}(g_{ni}|S_k) = \begin{cases} 1 & \text{if } S_k(n) = g_{ni}; \\ 0 & \text{otherwise.} \end{cases} \tag{13}$$

To evaluate the distribution $f_{S|X_e}(S_k|x_e)$ in Eq. (12), we assume that to make a decision given the measurement data, we have a non-conflicting threshold or boundary to make a prediction of the spring state, such that $f_{Y|X_e}(y_{n0}|x_e)$ and $f_{Y|X_e}(y_{n1}|x_e)$ do not intersect. This also implies $f_{G|X_e}(g_{ni}|x_e) = f_{Y|X_e}(y_{ni}|x_e)$. With this assumption, we have $f_{S|X_e}(S_k|x_e) = f_{A|X_e}(A_k|x_e)$.

We note that the quantity $f_{A|X_e}(A_k|x_e)$ is anti-causal, as it is asking for the true state of the springs when the measurement x_e is given. We use Bayes theorem to write it in a more desirable and causal form:

$$f_{A|X_e}(A_k|x_e) = \frac{f_{X_e|A}(x_e|A_k).f_A(A_k)}{\sum_{l=1}^{32} f_{X_e|A}(x_e|A_l).f_A(A_l)} = \frac{f_{X_e|A}(x_e|A_k)}{\sum_{l=1}^{32} f_{X_e|A}(x_e|A_l)}. \tag{14}$$

The likelihood $f_{X_e|A}(x_e|A_k)$ remains to be evaluated for all k. For a fixed collective spring state A_k, and a design e with $N_{\text{sg}}(e)$ number of strain gauges, $f_{X_e|A}(x_e|A_k)$ is the joint distribution of the $N_{\text{sg}}(e)$ strain measurements.

Although the true strain values of different strain-gauges are related due to the underlying physics, the noise in strain gauge measurements is taken to be statistically independent. We also assume (for modeling purposes) that the randomness in the strain gauge readings, primarily due to noise and uncertainties in loading, follows a Gaussian distribution. Let x_{en} represent the observed strain measurement in n-th strain-gauge of the design e, such that $x_e = \{x_{en}\}$ with $n \leq N_{\text{sg}}(e)$. For the selected spring state A_k and the design e, if x_{en}, μ_{en}, and σ_{en} represent the measurement of the strain gauge n (a random variable), its mean value, and the standard deviation respectively, we can write the following:

$$f_{X_e|A}(x_e|A_k) = \prod_{n=1}^{N_{\text{sg}}(e)} \frac{1}{\sqrt{2\pi\sigma_{en}^2}} \exp\left(-\frac{1}{2}\left(\frac{x_{en} - \mu_{en}}{\sigma_{en}}\right)^2\right) = \prod_{n=1}^{N_{\text{sg}}(e)} \frac{1}{\sigma_{en}} \phi\left(\frac{x_{en} - \mu_{en}}{\sigma_{en}}\right). \tag{15}$$

This gives us all the pieces to obtain $f_{G|X_e}(g_{ni}|x_e)$. We obtain the measurement data x_e using *Finite Element Model* (FEM) developed using OpenSees [38] or using a surrogate model developed using *Gaussian Process Regression* (GPR) [35].

We note that obtaining the likelihood $f_{X_e|A}(x_e|A_k)$ and the posterior $f_{A|X_e}(A_k|x_e)$ is not complicated for the chosen demonstration problem. Since our emphasis is more on the optimization framework, for simplicity we have assumed strain values to be uncorrelated and evaluation of the posterior can be done analytically as the decision space is discrete. However, for more complicated problems with correlated measurement values and continuous decision space, evaluation of the likelihood and the posterior will be more involved. For instance, in such cases, we use numerical techniques like *Markov Chain Monte Carlo* (MCMC), *Sequential Monte Carlo* (SMC) (refer to

[41]), or other methods to evaluate posterior.

Remark 1: We note that the *true* strain values of different strain gauges are correlated (or functionally related) by the underlying physics of the problem. That is, each of the strain gauge readings embeds some information about the state of the structure. In this paper, we use the Finite Element Model (FEM) as the *ground truth* (discussed more in the next section). This implies that the strain values obtained from the FEM are treated as the *actual/true* strain measurement that is impossible to be known since there will always be noise in *observed* strain readings. For a given load condition, we have a deterministic prediction of the mean value of the strain reading using the FEM model (or the respective digital surrogate constructed using strain data obtained from the FEM) which is considered to be the ground truth. However, the noise in the various strain gauge reading is statistically independent since the noise pertains to a given strain gauge itself. In this paper, we have assumed a Gaussian structure to the noise.

4.2 Finite element and Surrogate model

Section 3 details the finite element model of the structure of interest built using shell elements. We consider that the loading in the beam is uncertain, such that, the concentrated load $p \in \Omega_P$ and its locations $p_{\text{loc}} \in \Omega_{P_{\text{loc}}}$ is represented by the random variables P and P_{loc} respectively. We run the FE model for 5000 samples of random input data consisting of seven quantities: the true state of the springs $A_k \in A$ (consisting of states of 5 springs), the magnitude of the load $P \sim N(\mu_p = 1000 \text{ newton}, \sigma_p = 100 \text{ newton})$, and the location of the load $P_{\text{loc}} \sim HN(\mu_{\text{loc}} = 10\ m, \sigma_{\text{loc}} = 1\ m)$. Here, $HN(\cdot, \cdot)$ represents the half normal distribution. For each input sample, we obtain 22,500 strain responses. From here on Ω_Z represent the space of input sample, such that $z \in \Omega_Z$.

We would like to note that in many machine learning problems, physics-based models are unavailable, and the engineers must rely on fitting a numerical model using the data obtained from the experiments. In our case, we obtain the data from the finite element model, which we consider as "ground truth". Although we have the luxury of utilizing the finite element model, the computational cost is restrictive, and therefore, not the best option with which to carry out Bayesian optimization. For Bayesian calibration, metamodels or surrogate models are preferable, e.g., Support Vector Regression (SVR) [42], Gaussian Process Regression (GPR) [42, 35], Neural Network [43], and Polynomial Chaos Expansion (PCE) [44]. Models like PCE and SVR yield a point prediction of the output. Therefore, they are computationally cheaper than approaches like GPR that also predicts the uncertainties in the output. We use GPR to build our surrogate model which turns out to be 5000 times faster than the FEM model. The output of the surrogate model usually has a very large dimension. We overcome the issue of high-dimensional output space using the *Single Value Decomposition* (SVD) technique that reduces the high-dimensional correlated output space to low-dimensional uncorrelated features. We transform the strain response from 22500 dimensions to lower 28-dimensional latent space using SVD. These 28 important features cover 99.2% of the

total information of the data. These 28 features can be inverted to obtain the complete strain gauge response. We have built the surrogate model for each of these 28 features using GPR. One-third of the 5000 data points were used for training the GPR, whereas, the remaining Two-third was used for validation to verify the accuracy of the surrogate. Fig. 4 illustrates the discussion carried out so far.

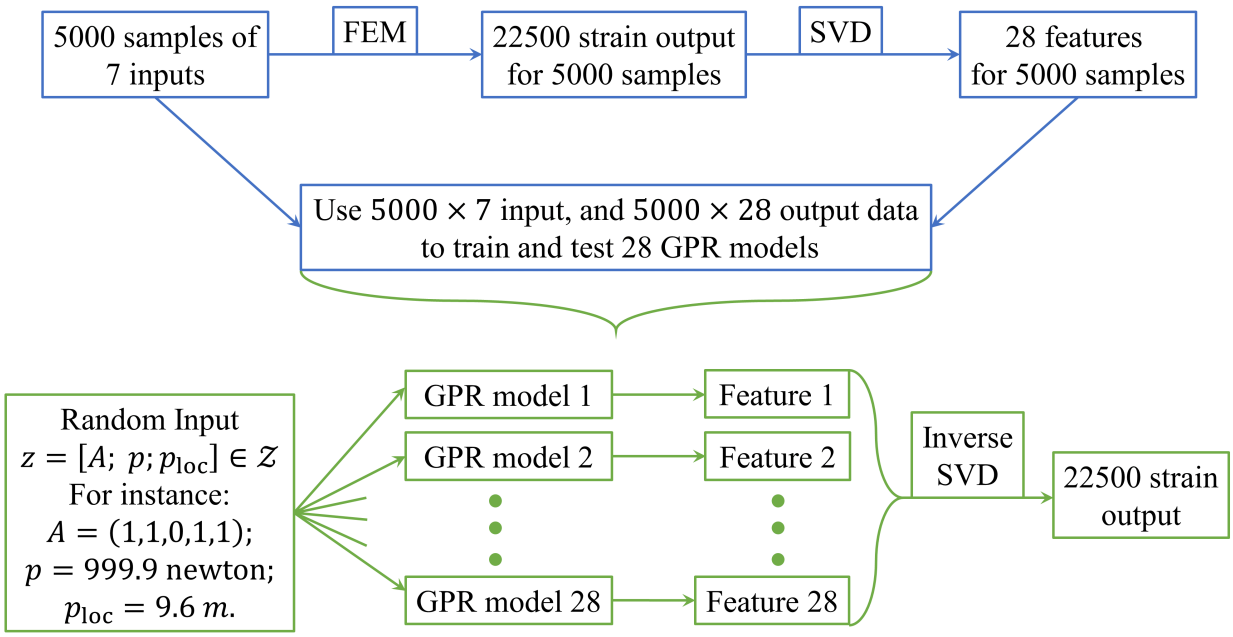

Figure 4: Flowchart describing strain data generation using FEM, and prediction using GPR surrogate model

The Figures 5a and 5b show the nearly identical strain field obtained for FEM and the surrogate model for a random input sample. Fig. 6a shows the error in the prediction of the strain values using the FEM and GPR model for the bottom 100 strain gauge locations at the left boundary of the beam. Overall, the absolute prediction error is of the order 10^{-7}, and the relative error is of the order 10^{-3}. However, a relatively high prediction error is observed at the locations of springs. Similarly, Fig. 6b shows the distribution of the absolute prediction error across the beam for a random input sample. Once again, relatively higher errors are observed at the spring locations and the location where the concentrated load acts.

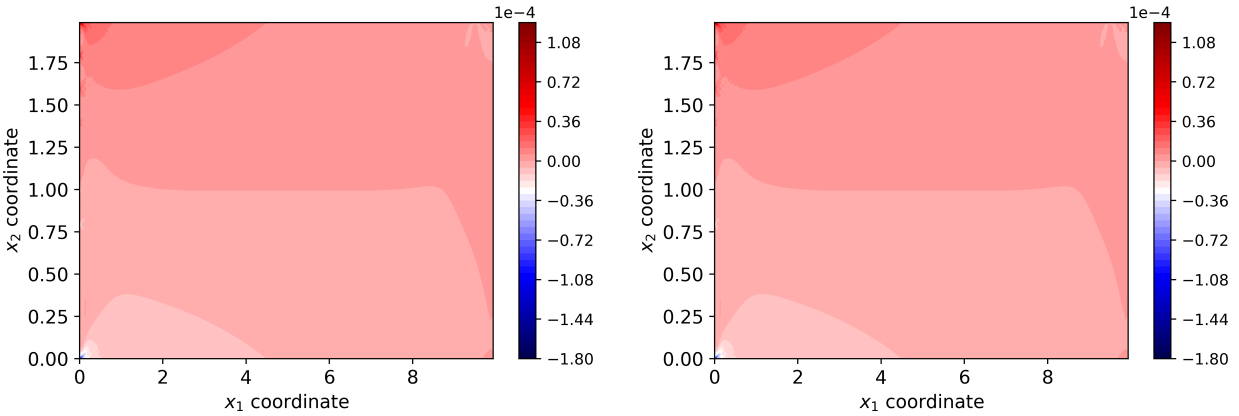

(a) Strain field obtained using FEM

(b) Strain field obtained using GPR model

Figure 5: Comparison of the strain fields obtained using FEM and GPR model

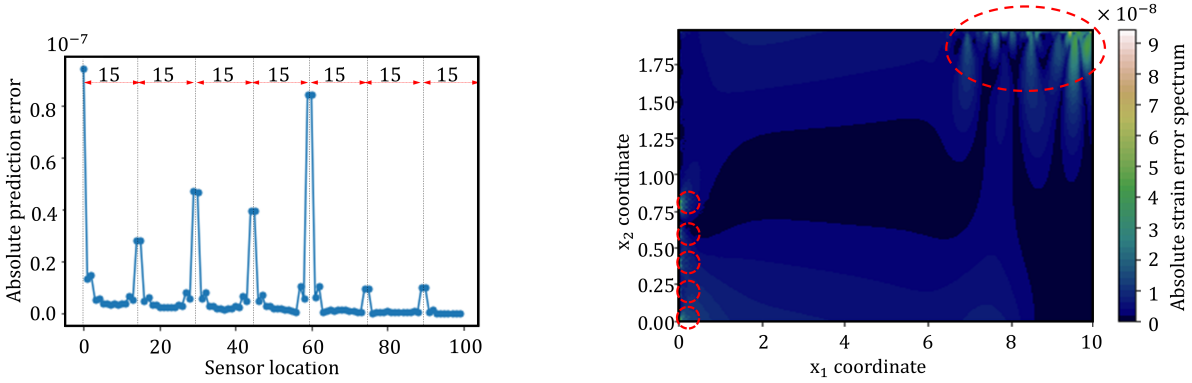

(a) Error in the 100 strain values at the left boundary of the beam

(b) Error in the strain values for a random input sample

Figure 6: Error in the strain values obtained using FEM and GPR model

4.3 Revisiting Bayes risk

As seen in Section 4.2, the measurement $x_e \in \Omega_{X_e}$ depends on the load $p \in \Omega_P$, its location $p_{\text{loc}} \in \Omega_{P_{\text{loc}}}$. The randomness in the strain values (observations) $x_e \in \Omega_{X_e}$ are primarily due to the noise in strain gauge, uncertainties in the concentrated load, and its location. We assume a zero mean Gaussian noise structure $\zeta \sim N(\mu_\varepsilon = 0,\ \sigma_\varepsilon = 5 \times 10^{-7})$. Let ε represent the realization of noise and Ω_ζ represent the noise space, such that $\varepsilon \in \Omega_\zeta$.

Consider a design e with $N_{\text{sg}}(e)$ number of strain measurement locations. Let ζ_i represent the random variable for the noise in the i^{th} strain location. It is reasonable to assume that the $\big(N_{\text{sg}}(e) + 2\big)$ random variables $P,\ P_{\text{loc}},\ \zeta_i, \cdots,\ \zeta_{N_{\text{sg}}(e)}$ are statistically independent. We define a design dependent product space $\Omega_{\xi_e} = \Omega_P \times \Omega_{P_{\text{loc}}} \times \Omega_{\zeta_1} \times \Omega_{\zeta_2} \times \cdots \times \Omega_{\zeta_{N_{\text{sg}}(e)}}$. The random vector ξ_e consists of the realizations of the random variables $P,\ P_{\text{loc}},\ \zeta_i, \cdots,\ \zeta_{N_{\text{sg}}(e)}$. The joint density function

is then written as:

$$\begin{gathered} f_{\xi_e}(\beta) = f_P(p).f_{P_{\text{loc}}}(p_{\text{loc}}).\prod_{i=1}^{N_{\text{sg}}(e)} f_{\zeta_i}(\varepsilon_i),\ \text{where,} \\ \beta = \left(p \in \Omega_P, p_{\text{loc}} \in \Omega_{P_{\text{loc}}}, \varepsilon_1 \in \Omega_{\zeta_1}, \varepsilon_2 \in \Omega_{\zeta_2}, \cdots, \varepsilon_{N_{\text{sg}}(e)} \in \Omega_{\zeta_{N_{\text{sg}}(e)}}\right) \in \Omega_{\xi_e}. \end{gathered} \tag{16}$$

Noting that the randomness in the measurement space Ω_{X_e} is by virtue of the uncertainty in Ω_{ξ_e} space, we rewrite Eq. (11) as follows,

$$f_{G|A}(g_{ni}|A_k) = \int_{\Omega_{\xi_e}} f_{G|\xi_e}(g_{ni}|\beta, A_k).f_{\xi_e}(\beta)\,\mathrm{d}\beta \ \text{ where,} \tag{17a}$$

$$f_{G|\xi_e}(g_{ni}|\beta, A_k) = f_{G|X_e}(g_{ni}|x). \tag{17b}$$

The second equation holds because a fixed input sample z, and noise value, yields a determinate and unique value of the measurement $x \in \Omega_{X_e}$. Substituting Eq. (17) into Eq. (10) yields:

$$\Psi_{\text{design-ex}}(e) = \int_{\Omega_{\xi_e}} \sum_{k=1}^{32} \mathscr{L}(\beta, A_k; e) f_A(A_k) f_{\xi_e}(\beta) d\beta,\ \text{where,} \tag{18a}$$

$$\mathscr{L}(\beta, A_k; e) = \sum_{n=1}^{5}\sum_{i=0}^{1} w_n L\left(g_{ni}, A_k\right) f_{G|\xi_e}(g_{ni}|\beta, A_k). \tag{18b}$$

We note that these random variables constituting β can follow a generic distribution. We can always transform them to a standard normal random variables. Therefore, in an attempt to generalize, we transform the load P, its location P_{loc}, and the noise ζ_i into their respective standard normal forms. Since the load and the noise for the i^{th} strain gauge is Gaussian in our case, their standard normal forms can be written as $\mathscr{U}$ (standard normal counterpart of P), and $\mathscr{V}_i$ (standard normal counterpart of ζ_i), such that $p = u\sigma_p + \mu_p$, and $\varepsilon_i = v_i\sigma_\varepsilon + \mu_\varepsilon$, where u and v_i are the realizations of $\mathscr{U}$, and $\mathscr{V}_i$ respectively. We transform $f_{P_{\text{loc}}}(p_{\text{loc}})$ from *Half Normal* to a *Standard Normal* random variable $\mathscr{U}_{\text{loc}}$, such that the cumulative density functions are equal: $F_{P_{\text{loc}}}(p_{\text{loc}}) = F_{\mathscr{U}_{\text{loc}}}(u_{\text{loc}})$, and $\mu_{p_{\text{loc}}} = F^{-1}_{P_{\text{loc}}}\left(F_{\mathscr{U}_{\text{loc}}}(\mu_{u_{\text{loc}}})\right)$. This transforms ξ_e into a joint standard normal random variable $\mathscr{B}_e$ (with a realization $\mathscr{b}$, where $\mathscr{b} \in \Omega_{\mathscr{B}_e}$), such that

$$\begin{gathered} f_{\mathscr{B}_e}(\mathscr{b}) = f_{\mathscr{U}}(u).f_{\mathscr{U}_{\text{loc}}}(u_{\text{loc}}).\prod_{i=1}^{N_{\text{sg}}(e)} f_{\mathscr{V}_i}(v_i),\ \text{where,} \\ \mathscr{b} = \left(u, u_{\text{loc}}, v_1, v_2, \cdots, v_{N_{\text{sg}}(e)}\right). \end{gathered} \tag{19}$$

We can now rewrite Eq. (18) as:

$$\Psi_{\text{design-ex}}(e) = \int_{\Omega_{\mathscr{B}_e}} \sum_{k=1}^{32} \lambda(\mathscr{E}, A_k; e) f_A(A_k) f_{\mathscr{B}_e}(\mathscr{E}) \mathrm{d}\mathscr{E}, \text{ where,} \tag{20a}$$

$$\lambda(\mathscr{E} = (u, u_{\text{loc}}, v_i), A_k; e) = \mathscr{L}\left(\beta = \left(u\sigma_p + \mu_p,\ F^{-1}_{P_{\text{loc}}}\left(F_{\mathscr{U}_{\text{loc}}}(u_{\text{loc}})\right),\ v_i\sigma_\varepsilon + \mu_\varepsilon, A_k; e\right)\right). \tag{20b}$$

Section 4.4 deals with evaluating the Bayes risk discussed in this section. To maintain generality, we present the formula for Bayes risk as an approximation of both, Eq. (18a), and Eq. (20a).

4.4 Evaluating the expected cost considering uncertainties in load and noise in the observed strains

4.4.1 Obtaining the cost $\mathscr{L}$ for a given input sample z and noise structure

Once we have the GPR models, we can obtain $f_{X_e|A}(x_e|A_k)$, and hence evaluate $f_{G|X_e}(g_{ni}|x_e)$ using Eq. (14). To demonstrate a simple case of the evaluation of posterior probability of spring existence, we ignore the uncertainties due to load and its location by fixing the load as: $p \in \Omega_P$ and $p_{\text{loc}} \in \Omega_{P_{\text{loc}}}$. We consider a design with $N_{\text{sg}}(e)$ strain gauges, picked randomly using *Latin Hypercubic Sampling*. Assuming that the true state of the springs is A, we consider the input sample as $z = (A;\ p;\ p_{\text{loc}}) \in \Omega_Z$. For the chosen design e and the input sample z, we run multiple surrogate runs over different noise values in the Monte Carlo sense. The posterior can then be obtained using Eq. (15). Similarly, for the same fixed load and its location, the likelihood $f_{X_e|A}(x_e|A_k)$ for all possible spring states can be obtained, yielding $f_{A|X_e}(A_k|x_e)$ using Eq. (16). Finally, we can obtain $f_{G|X_e}(g_{ni}|x_e)$ using equations(12) and (13). Equations (17b) and (18b) yields $\mathscr{L}(\beta,\ A_k; e)$. Fig. 7 illustrates the discussion so far.

For this special example with a fixed load and its location, and that we have assumed a well defined noise structure with zero mean $\zeta \sim N(0, 5\times10^{-7})$, we can obtain the likelihood $f_{X_e|A}(x_e|A_k)$ without numerous surrogate runs. For the fixed input sample z, let $\bar{x}_{ei}$ represent the strain values at the n-th sensor locations obtained using either a forward FEM or a surrogate model. The closed form likelihood for such case can then be written as $f_{X_e|A}(x_e|A_k) = \prod_{n=1}^{N_{\text{sg}}(e)} \frac{1}{5\times10^{-7}} \phi\left(\frac{x_{en}-\bar{x}_{en}}{5\times10^{-7}}\right)$.

We need to incorporate the cumulative uncertainties due to all the aforementioned entities into evaluating the Bayes risk. Evaluating $\Psi_{\text{design-ex}}(e)$ and calculating the associated integral in Eq. (18a) is computationally expensive and not so trivial. We do this by using three techniques discussed in the next section: a sampling-based approach, mean value approximation, and univariate dimension reduction with Gauss-Hermite quadrature.

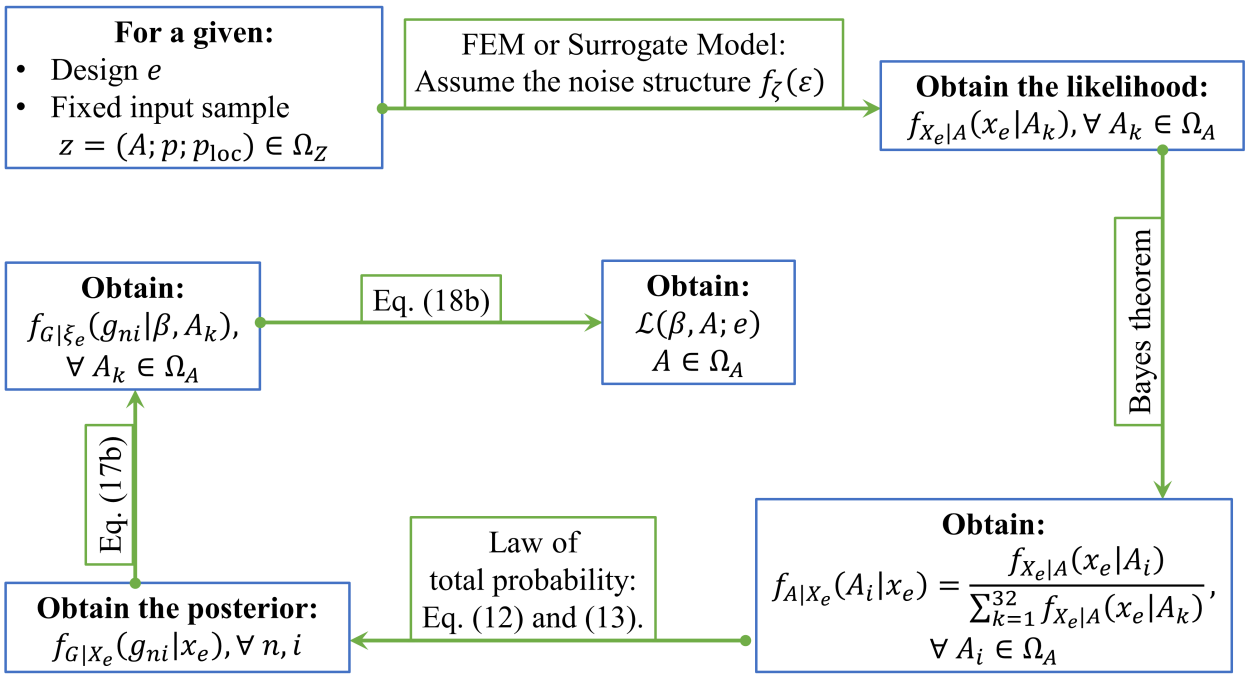

Figure 7: Flowchart describing the approach to obtain the cost $\mathscr{L}$ for a given design e and input sample z

4.4.2 Approach 1: Sampling-based method

This is a Monte Carlo based approach, where we generate large number of random samples of $A_i \in \Omega_A$, and $\beta_i \in \Omega_{\xi_e}$, with $i \in \{1, 2, 3, \cdots, N_{\text{mcs}}\}$. Here, N_{mcs} denotes the number of Monte Carlo samples. For the design e, we can obtain the cost $\mathscr{L}(\beta_i,\ A_i; e)$ for each A_i and β_i similar to the procedure detailed in previous Section 4.4.1. The Bayes risk is then approximated as:

$$\Psi_{\text{design-ex}}(e) \approx \frac{1}{N_{\text{mcs}}} \sum_{i=1}^{N_{\text{mcs}}} \mathscr{L}(\beta_i,\ A_i; e) \tag{21a}$$

$$\Psi_{\text{design-ex}}(e) \approx \frac{1}{N_{\text{mcs}}} \sum_{i=1}^{N_{\text{mcs}}} \lambda(\mathscr{C}_i,\ A_i; e). \tag{21b}$$

The approximated Bayes risk depicted in the above equations is also called *empirical risk*. We recall here that Eq. (21a) and (21b) represents the approximated Bayes risk corresponding to Eq. (18), and Eq. (20) respectively. Fig. 8 illustrates a convergence plot for the sampling-based method obtained for a design e, with $N_{\text{sg}}(e) = 30$ strain gauges. The expected cost converges to 327.2 (showed by the red line) around $N_{\text{mcs}} = 10000$ samples with the average noise of 0.71. However, the evaluation of Bayes risk for 10000 samples takes 265 seconds. The optimization process demands an evaluation of the cost function around ten thousand times. Therefore, the sampling-based method is computationally expensive.

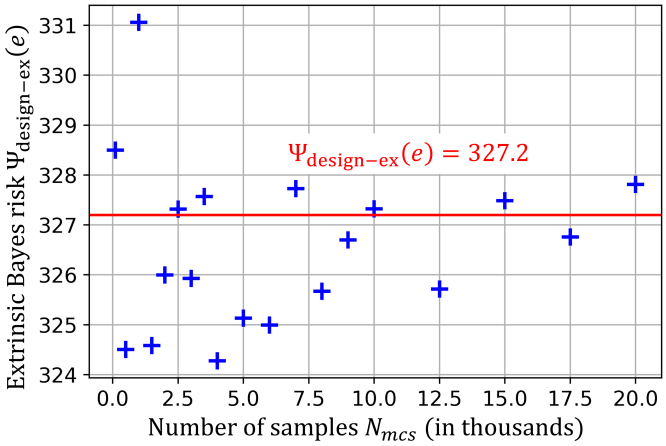

Figure 8: Convergence plot of Bayes risk obtained using sampling-based method

4.4.3 Approach 2: Mean value approximation

Here, we evaluate the Bayes risk as the cost $\mathscr{L}(\beta,\ A_k; e)$ evaluated for all the spring states A_k at the mean value of the load, its location, and noise, weighted over by the probability $f_A(A_k)$, such that:

$$\Psi_{\text{design-ex}}(e) \approx \sum_{k=1}^{32} \mathscr{L}\left(\beta = \left(\mu_p,\ \mu_{p_{\text{loc}}},\ \mu_{\varepsilon_1},\ \mu_{\varepsilon_2}, \cdots,\ \mu_{\varepsilon_{N_{\text{sg}}(e)}}\right),\ A_k; e\right) f_A(A_k); \tag{22a}$$

$$\Psi_{\text{design-ex}}(e) \approx \sum_{k=1}^{32} \lambda\left(\mathscr{b} = \left(\mu_u,\ \mu_{u_{\text{loc}}},\ \mu_{v_1},\ \mu_{v_2}, \cdots,\ \mu_{v_{N_{\text{sg}}}}\right),\ A_k; e\right) f_A(A_k). \tag{22b}$$

Since, $\mathscr{U}$, $\mathscr{U}_{\text{loc}}$, and $\mathscr{V}_i$ are standard normal random variables, we have $\mu_u = 0;\ \mu_{u_{\text{loc}}} = 0;\ \mu_{v_i} = 0$, $\forall i \leq N_{\text{sg}}(e)$.

4.4.4 Approach 3: Univariate dimensional reduction with Gauss-Hermite quadrature

Approach 1 is computationally expensive as it involves considering a large sample size, whereas approach 2 is feasible but not very accurate when there is large variability. We tackle these limitations using the current approach to evaluate Bayes risk.

We assume a design e, with $N_{\text{sg}}(e)$ number of strain gauges. We start by redefining Bayes risk in Eq. (20) as:

$$\Psi_{\text{design-ex}}(e) = \int_{\Omega_{\mathscr{B}_e}} h(\mathscr{b}; e) f_{\mathscr{B}_e}(\mathscr{b}) \mathrm{d}\mathscr{b},\ \text{where,} \tag{23a}$$

$$h(\mathscr{b}; e) = \sum_{k=1}^{32} \lambda(\mathscr{b}, A_k; e) f_A(A_k). \tag{23b}$$

Recall, that the vector $\mathscr{b} = (u, u_{\text{loc}}, v_1, v_2, \cdots, v_{N_{\text{sg}}}(e))$ consist of $\left(N_{\text{sg}}(e) + 2\right)$ variables. We now

define the following vectors consisting of $\left(N_{\text{sg}}(e)+2\right)$ elements:

$$\begin{aligned}
b_0 &= (0,0,0,0,\cdots,0);\\
b_1 &= (u,0,0,0,\cdots,0);\\
b_2 &= (0,u_{\text{loc}},0,0,\cdots,0);\\
b_3 &= (0,0,v_1,0,\cdots,0);\\
b_4 &= (0,0,0,v_2,\cdots,0);\\
&\vdots\\
b_{\left(N_{\text{sg}}(e)+2\right)} &= (0,0,0,0,\cdots,v_{N_{\text{sg}}(e)}).
\end{aligned} \tag{24}$$

Using the definitions above and *univariate dimensional reduction* (refer to [45]), we approximate the function $h(\mathscr{E};e)$ as:

$$h(\mathscr{E};e) \approx -\left(N_{\text{sg}}(e)+1\right)\lambda(b_0,A_k;e) + \sum_{i=1}^{\left(N_{\text{sg}}(e)+2\right)} \lambda(b_i,A_k;e). \tag{25}$$

Substituting Eq. (25) into Eq. (23), we get,

$$\Psi_{\text{design-ex}}(e) \approx \sum_{k=1}^{32}\left(-\left(N_{\text{sg}}(e)+1\right)\lambda(b_0,A_k;e) + \sum_{i=1}^{\left(N_{\text{sg}}(e)+2\right)}\int_{\Omega_{\mathscr{B}_e}} \lambda(b_i,A_k;e) f_{\mathscr{B}_e}(\mathscr{E})\mathrm{d}\mathscr{E}\right) f_A(A_k). \tag{26}$$

To simplify the expression above, firstly, we realize that $f_{\mathscr{B}_e}(\mathscr{E})$ is the joint probability density function of statistically-independent standard normal random variables. Therefore,

$$f_{\mathscr{B}_e}(\mathscr{E}) = \phi(u).\phi(u_{\text{loc}}).\prod_{i=1}^{N_{\text{sg}}(e)}\phi(v_i) = \prod_{i=1}^{N_{\text{sg}}(e)+2}\phi(\mathscr{E}_i) = \prod_{i=1}^{N_{\text{sg}}(e)+2}\left(\frac{1}{\sqrt{2\pi}}e^{-\frac{1}{2}\mathscr{E}_i^2}\right). \tag{27}$$

In the equation above, $\mathscr{E}_1 = u$, $\mathscr{E}_2 = u_{\text{loc}}$, and $\mathscr{E}_{j+2} = v_j$, for $j \in (1,2,\cdots,N_{\text{sg}}(e))$. Secondly, we note that for any function of the form $g(x,y)$, $E_{XY}(g(x,0)) = E_X(g(x,0))$, provided X and Y are statistically-independent random variables. This allows us to simplify the integral in Eq. (26) as:

$$\int_{\Omega_{\mathscr{B}_e}} \lambda(b_i,A_k;e) f_{\mathscr{B}_e}(\mathscr{E})\mathrm{d}\mathscr{E} = \frac{1}{\sqrt{2\pi}}\int_{\mathscr{E}_i} \lambda(b_i,A_k;e)e^{-\frac{1}{2}\mathscr{E}_i^2}\mathrm{d}\mathscr{E}_i. \tag{28}$$

We realize that the Gauss-Hermite quadrature is a natural choice for approximating integral in the equation above. This is because Gauss-Hermite quadrature is meant to estimate integrals of form

$\int g(x)e^{-x^2}\,\mathrm{d}x$, for any function g(x). Therefore, the integral above is approximated as:

$$\int_{\mathscr{E}} \lambda(b_i, A_k; e) f_{\mathscr{B}_e}(\mathscr{E}) \mathrm{d}\Omega_{\mathscr{B}_e} \approx \frac{1}{\sqrt{\pi}} \sum_n w_n \lambda(q_{i,n}, A_k; e);$$
$$q_{i,n}(j) = \begin{cases} b_i(j) = 0 & i \neq j; \\ \sqrt{2}\alpha_n & i = j. \end{cases} \tag{29}$$

In the equation above, n represents quadrature order, w_n gives the weights, and α_n gives the point of evaluation of the function. For our calculations, we use $n = 2$, for which $w_n = 0.5\sqrt{\pi}$, and $\alpha_n = \pm\frac{1}{\sqrt{2}}$. The approximated Bayes risk can now be written as:

$$\Psi_{\text{design-ex}}(e) \approx \sum_{k=1}^{32} \left(-\left(N_{\text{sg}}(e) + 1\right) \lambda(b_0, A_k; e) + \sum_{i=1}^{\left(N_{\text{sg}}(e)+2\right)} \sum_n w_n \lambda(q_{i,n}, A_k; e) \right) f_A(A_k). \tag{30}$$

The advantage of Bayes risk expressed in the form of Eq. (20) is clear from the discussion carried out so far. The expression of Bayes Risk in Eq. (30) can easily be extended to obtain Bayes risk in the form of Eq. (18).

The table below compares the value of Bayes risk and the run time for various approaches discussed in this section. The sampling-based method is the most accurate when a large sample size is considered. However, it is computationally expensive. Secondly, irrespective of the sample size, the Bayes risk approximated using approach 1 changes with the new sample even with the same sample size, hence, is random and non-unique. Approach 2 is the most feasible but not so accurate. Approach 3 enjoys acceptable accuracy and computational speed.

	Bayes risk $\Psi_{\text{design-ex}}(e)$	Run time in seconds
Approach 1 (10^4 samples)	327.32	229.97
Approach 2	309.81	0.82
Approach 3	321.35	46.53

Table 3: Comparison of various approaches in evaluating Bayes risk for a design e with $N_{\text{sg}}(e) = 30$

The discussion in the paper so far was about evaluating the Bayes risk for a given design e. The next section focus on the problem of optimal sensor placement using Bayesian optimization. We use *approach 3* to evaluate the extrinsic Bayes risk $\Psi_{\text{design-ex}}(e)$ and assume an intrinsic cost of unity per additional sensor.

5 Bayesian optimization: Optimal sensor placement design

5.1 Optimal sensor placement design algorithm

Our primary objective is to obtain the optimal sensor placement design e^* that minimizes the Bayes risk functional discussed in the previous sections. Mathematically,

$$e^* = \arg\min_{e} \Psi_{\text{design}}(e) \in \Omega_E. \tag{31}$$

In absolute terms, obtaining e^* involves looking at every possible design combination, and picking the one with the least Bayes risk. In our case, if $n = 22500$, this would be picking e^* from the $\sum_{r=1}^{n} \frac{n!}{r!(n-r)!} = (2^n - 1)$ possible combinations of sensor locations. Clearly, sampling the entire design space Ω_E, which consists of $(2^{22500} - 1) \approx 10^{6773}$ number of possible designs, is daunting even for this modest problem. The main motivation of using Bayesian optimization is to arrive at the optimal solution e^* by minimizing the sampling points to fasten the optimization process. Bayesian optimization looks for the global optimum in a minimum number of steps.

Unlike gradient-based optimization methods, Bayesian optimization is a global optimization technique that does not require the derivative of the objective function. Having a black-box model (like a surrogate function) of the objective function suffices to perform the optimization. It involves two primary elements. The first element is developing *surrogate function* using *Gaussian process regression* (GPR) of the objective function using randomly evaluated sample. Consider, for example in our case, we assume an initial design $e_0 \in \Omega_E$, with 3 strain locations. To obtain the next optimal design with 4 strain gauges, we randomly sample, for instance, 20 locations to be the candidate for the 4^{th} sensor. These locations yield 20 design samples $\tilde{e}(k),\ \forall\ k \leq 20$ each with four sensors. We obtain the exact cost $\Psi_{\text{design}}(\tilde{e}(k)),\ \forall\ k \leq 20$ using approach 3 discussed in previous section. Using the 20 set input data of the fourth sensor location $\mathscr{d} = (x_1, x_2)$, and the output data of the exact cost, we train our surrogate function $\hat{\Psi}_{\text{design}}(\mathscr{d}) \sim N(\mu_{\mathscr{d}}, \sigma_{\mathscr{d}})$. It provides a posterior probability that describes possible values for the cost at a candidate fourth location $\mathscr{d}$, with the mean value $\mu_{\mathscr{d}}$, and the standard deviation $\sigma_{\mathscr{d}}$. The second component is the *acquisition function* that helps us locate the next *most valuable* candidate for the fourth location based on the current posterior over the cost. We use *Expected Improvement EI* as our acquisition function.

$$EI(\mathscr{d}) = \left(\mu_{\mathscr{d}} - \Psi^*_{\text{design}}\right) \Phi\left(\frac{\mu_{\mathscr{d}} - \Psi^*_{\text{design}}}{\sigma_{\mathscr{d}}}\right) + \sigma_{\mathscr{d}} \phi\left(\frac{\mu_{\mathscr{d}} - \Psi^*_{\text{design}}}{\sigma_{\mathscr{d}}}\right). \tag{32}$$

Here, $\Psi^*_{\text{design}} = \min_{\tilde{e}(k)} \Psi_{\text{design}}(\tilde{e}(k))$ is the *current best values* of the objective function. For all the remaining $(22500 - 20 - 3) = 22477$ possible fourth location candidates, we evaluate $EI(\mathscr{d})$. The candidate with maximum *EI* is the next most valuable location. Once we locate the next most valuable fourth location candidate, we get 21^{st} design sample. We re-train the GPR with 21 data points, and keep adding the next most valuable location until the maximum *EI* is less than a tolerance

value ε. For detailed understanding of Bayesian optimization, readers are recommended to refer to [33] and [35].

To generalize our optimization algorithm, we define the initial sensor design as $e_0 \in \Omega_E$, with $N_0 = N_{\text{sg}}(e_0)$ number of strain gauges. If $\mathscr{A}^{(i)} = (x_1^{(i)}, x_2^{(i)})$ represents the location of i^{th} strain gauge ($x_1^{(i)}$ and $x_2^{(i)}$ denote the horizontal and vertical coordinates of the sensor i), we have $e_0 = \left(\mathscr{A}^{(1)}, \mathscr{A}^{(2)}, \cdots, \mathscr{A}^{(N_0)}\right)$. Let N_{as} represent number of additional sensors that will be added one by one to N_0 during the optimization process. Let $e_{n_{\text{as}}}$ represent the optimized sensor design with $\left(N_0 + n_{\text{as}}\right)$ sensors, such that $n_{\text{as}} \leq N_{\text{as}}$, and $e^* = \arg\min_{e_{n_{\text{as}}}} \Psi_{\text{design}}(e_{n_{\text{as}}})$. Finally, $N_{\text{total}} = 22500$ represents total number of strain gauge locations. Fig. 9 details the flowchart of the optimization algorithm 1 developed for obtaining optimal sensor placement. In Yang et al. [46], this algorithm was deployed to obtain a sensor placement design of a more complex real-world miter gate structure that had a different type of damage (unlike the detection type of problem here) and a different Bayes risk functional (quantifying the net relative gain in information). It shows the generality and applicability of the proposed algorithm.

Algorithm 1: Bayesian optimization for sensor placement

Initialize $e_0 = \left(\mathscr{d}^{(1)}, \mathscr{d}^{(2)}, \cdots, \mathscr{d}^{(N_0)}\right)$;

for $n_{as} = 1$ **to** N_{as} **do**

  Using LHS, randomly select α locations to be candidates for the $(N_0 + n_{\text{as}})$ sensor location, with coordinates $\mathscr{X} = \left(\tilde{\mathscr{d}}^{(1)}, \tilde{\mathscr{d}}^{(2)}, \cdots, \tilde{\mathscr{d}}^{(\alpha)}\right)$;

  Obtain α number of possible designs: $\tilde{e}_k = \text{concatenate}\left(e_{(n_{\text{as}}+1)}, \tilde{\mathscr{d}}^{(k)}\right)$, for all $k \leq \alpha$;

  Obtain the exact cost of all the α designs: $\Xi = \left(\Psi_{\text{design}}(\tilde{e}_1), \Psi_{\text{design}}(\tilde{e}_2), \cdots, \Psi_{\text{design}}(\tilde{e}_\alpha)\right)$;

  while $i = 1$ **or** $maxEI < \varepsilon$ **do**

    Construct the GPR model for $\hat{\Psi}_{\text{design}}(\cdot)$ trained using (X, Ξ);

    For all the remaining strain locations $Z = \left(\bar{\mathscr{d}}^{(1)}, \bar{\mathscr{d}}^{(2)}, \cdots, \bar{\mathscr{d}}^{(\beta)}\right)$, where $\beta = \left(N_{\text{total}} - \left(N_0 + n_{\text{as}} - 1\right) - \alpha\right)$, obtain β number of possible designs: $\bar{e}_m = \text{concatenate}\left(e_{(n_{\text{as}}+1)}, \bar{\mathscr{d}}^{(m)}\right)$, for all $m \leq \beta$;

    Obtain the cost $\hat{\Psi}_{\text{design}}\left(\bar{\mathscr{d}}^{(m)}\right)$ for all $m \leq \beta$ designs using GPR developed before;

    Obtain the currrent best $\Psi^*_{\text{design}} = \min \Xi$;

    Obtain the Expected Improvement for all the β designs using:

$$EI(\bar{\mathscr{d}}^{(m)}) = \left(\mu_{\bar{\mathscr{d}}^{(m)}} - \Psi^*_{\text{design}}\right) \Phi\left(\frac{\mu_{\bar{\mathscr{d}}^{(m)}} - \Psi^*_{\text{design}}}{\sigma_{\bar{\mathscr{d}}^{(m)}}}\right) + \sigma_{\bar{\mathscr{d}}^{(m)}} \phi\left(\frac{\mu_{\bar{\mathscr{d}}^{(m)}} - \Psi^*_{\text{design}}}{\sigma_{\bar{\mathscr{d}}^{(m)}}}\right)$$

    , where $m \leq \beta$;

    Obtain:

$$maxEI = \max_{\bar{\mathscr{d}}^{(m)}} \left(EI(\bar{\mathscr{d}}^{(m)})\right)$$

$$\bar{\mathscr{d}} = \arg\max_{\bar{\mathscr{d}}^{(m)}} \left(EI(\bar{\mathscr{d}}^{(m)})\right)$$

$$\bar{e} = \text{concatenate}\left(e_{(n_{\text{as}}+1)}, \bar{\mathscr{d}}\right)$$

    Evaluate the exact cost $\mathfrak{E}(\bar{e})$;

    Update:

$$\mathscr{X} = \text{concatenate}\left(\mathscr{X}, \bar{\mathscr{d}}\right)$$

$$\tilde{e}_{(\alpha+i)} = \bar{e}$$

$$\Xi = \text{concatenate}\left(\Xi, \Psi_{\text{design}}(\bar{e})\right)$$

    $i = i + 1$;

  end

  Update the sensor design: $e_{n_{\text{as}}} = \text{concatenate}(e_{n_{\text{as}}-1}, \bar{\mathscr{d}})$;

end

Obtain: $e^* = \arg\min_{e_k} \Psi_{\text{design}}(e_k)$, where, $k \leq N_{\text{as}}$;

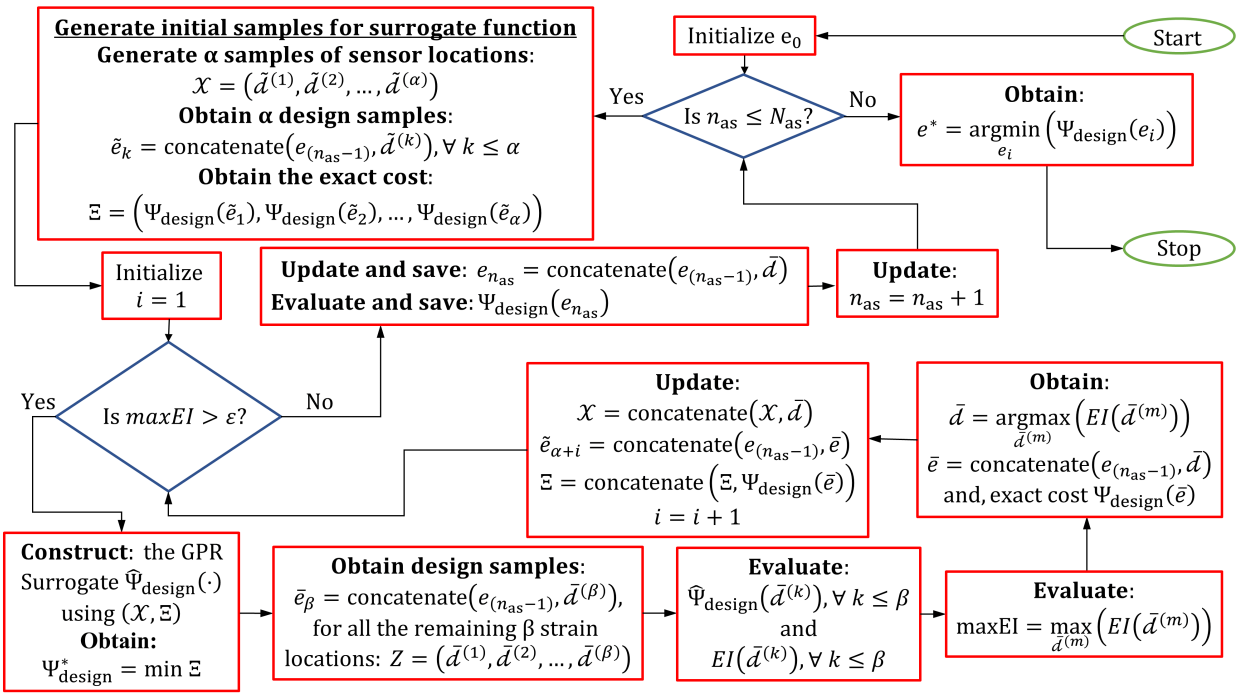

Figure 9: Flowchart of Bayesian optimization algorithm for optimal sensor placement design

5.2 Results and discussion

5.2.1 Comparison of a Bayesian optimized sensor placement design with randomly-chosen designs

To numerically implement the optimization algorithm discussed in Section 5.1, we consider an initial design e_0 with $N_0 = 3$, with sensors picked randomly, and consider $N_{as} = 10$ additional sensors. We fix $\alpha = 20$. Fig. 10a below shows the sensors constituting e_0 by blue dots and the additional sensor location by red dots placed on the strain contour (for a random input sample) of the beam. For instance, the design e_1 consists of all the three initially considered sensors along with the fourth sensor in red (marked by number 4). Fig. 10a also shows the strain field for a realization of load and its location. Fig. 10b illustrates Bayes risk for the designs $e_{n_{as}}$. We observe that the Bayes risk converges with 4 additional sensor, i.e., e_4 can be considered as the optimal design. We also observe that almost all these additional sensors are concentrated close to the boundary where the springs are present. We observe in all the following convergence plots (Figures 10b, 13b- 17b) that the Bayes risk increases after the minimum value is attained because every additional sensor bears an intrinsic cost, which in this case was assumed to be unity per additional sensor.

To demonstrate the fact that Bayesian optimization produces the optimal sensor placement design, we consider a random design e_r, with $N_{sg}(e_r) = 13$. Figure 11a shows the arrangement of the sensors for design e_r. Although design e_r has 6 more sensors than design e_4, the Bayes risk for e_r is much higher than that of the minimum Bayes risk for optimized design e_r. The reason is that the new information acquired by adding the 5-th sensor or more does not add to the value of

decision-making as much as it leads to the increase in the intrinsic cost due to the addition of more sensors. This is clear from Fig. 11b.

We used approach 3 to evaluate Bayes risk while performing Bayesian optimization. Fig. 12a and 12b, compare the expected cost obtained using the sampling-based method (approach 1, with 10^4 samples) and approach 3 for designs e_4 and e_r respectively. As expected, the results obtained using approach 3 are very close to the sampling-based method (that can be assumed as ground truth). The plots also show the *Kernel Density Estimate* (KDE) for the sampling-based method. Finally, the deviation of Bayes risk in the case of random design e_r as compared to the optimal design e_4 is noteworthy.

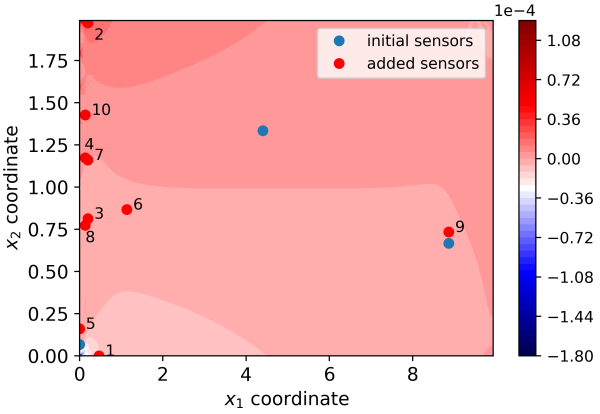

(a) Optimized sensor locations

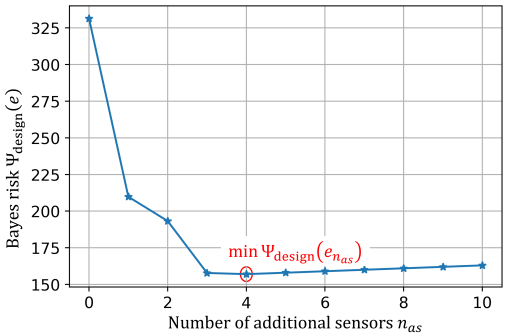

(b) Bayes risk

Figure 10: Optimized sensor placement and the associated Bayes risk obtained using approach 3

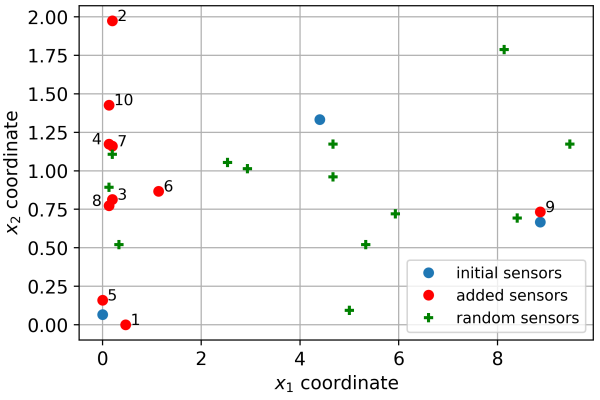

(a) Optimized sensor design $e_{n_{\text{as}}}$ and random design e_r

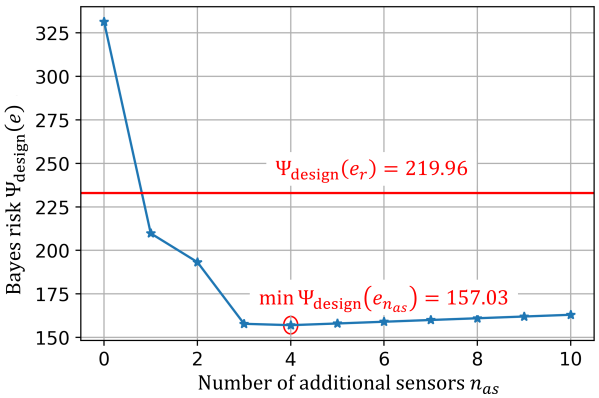

(b) Bayes risk $\Psi_{\text{design}}(e_{n_{\text{as}}})$ and $\Psi_{\text{design}}(e_r)$

Figure 11: Randomly selected sensor design e_r and the associated Bayes risk obtained using approach 3

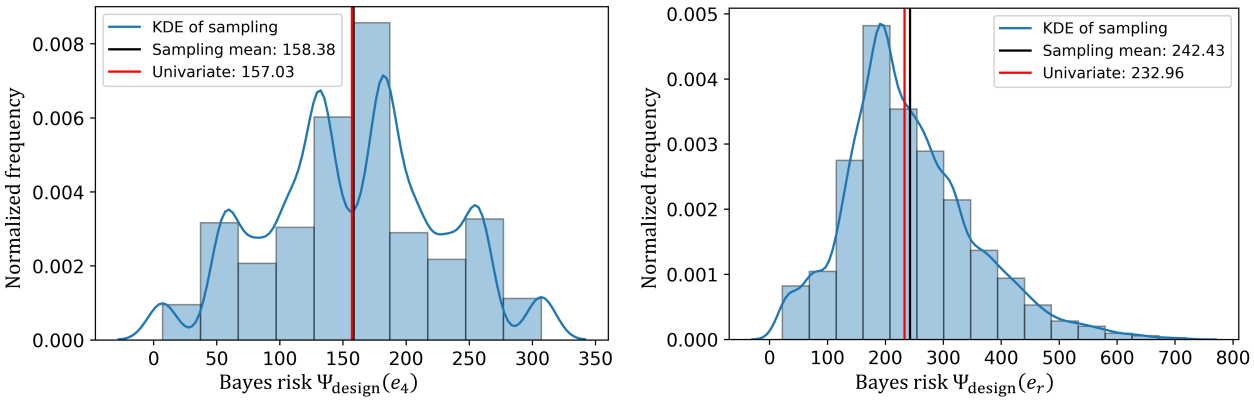

(a) For the optimized design e_4

(b) For the random design e_r

Figure 12: Comparison of the Bayes risk evaluated using sample-based method (approach 1), and univariate dimensional reduction technique (approach 3)

Remark 2: We note that obtaining new information (for example: strain gauge data) is consequential in making a better decision (for example: detecting the existence of springs). However, acquiring information through a mechanism e bears cost, represented by $\Psi_{\text{design-in}}(e)$. Acquiring the new information is meaningful and economical if and only if the additional cost required to gather the information is outweighed by the reduction in the expected losses evaluated by considering the additional information (see Chadha et al. [47]). Recall the expression of the Bayes risk $\Psi_{\text{design}}(e)$ in Eq. (9). The Bayes risk is defined as the sum of intrinsic cost $\Psi_{\text{design-in}}(e)$ and extrinsic cost $\Psi_{\text{design-ex}}(e)$. Increasing the number of sensors has the following effects:

1. Every addition of the sensor increases the cost due to the intrinsic cost of the sensor, cost incurred to install and maintain the SHM system. Therefore, $\Psi_{\text{design-in}}(e)$ increases.

2. Every addition of the sensor also adds to the new information about the state of the structure leading to better decision making. Therefore, with the increase in sensor count, $\Psi_{\text{design-ex}}(e)$ decreases.

With the addition of a new sensor up to the optimal design e^*, the $\Psi_{\text{design-ex}}(e)$ decreases more than the increase in $\Psi_{\text{design-in}}(e)$, leading $\Psi_{\text{design}}(e)$ to decrease overall. However, beyond the optimal design, with any new addition of the sensors, $\Psi_{\text{design-ex}}(e)$ decreases less than the increase in $\Psi_{\text{design-in}}(e)$, leading $\Psi_{\text{design}}(e)$ to increase overall. In other words, there comes a time when the benefit of the additional information obtained by adding an additional sensor is dwarfed by the cost incurred due to a sensor addition. This effect is observed in all the convergence plots presented in this section.

5.2.2 Comparison of a Bayesian optimized sensor placement design with Bayes risk evaluated using various approaches

We now focus on the performance of various approaches detailed in Section 4.4 used in evaluating the Bayes risk while performing Bayesian optimization. Figures 10, 13, and 14 illustrate

optimized sensor placement and the associated Bayes risk obtained using approaches 3, 1, and 2, respectively. It is not surprising that the convergence rate depends on the approach picked to evaluate the Bayes risk. Approach 2 (mean value approximation of Bayes risk) is not accurate, and the sampling-based method, like any Monte-Carlo based approach, bears uncertainties because it attempts to evaluate the integral in Bayes risk functional by sampling it. For a different sample with the same sample size, the Bayes risk evaluated using approach 1 is different. This randomness in the evaluation of Bayes risk using approach 1 leads the acquisition function to pick different sensor locations. Unlike these approaches, approach 3 attempts to evaluate the integral, and rather quickly and consistently (unlike sampling-based method), using Gaussian-Hermite quadrature. These inherent advantages of approach 3 catalyze the optimization code to converge faster. It can be observed that approach 3 finds the first 4 sensors to be well spread in the vertical direction. The first four additional sensor locations obtained by using the Sampling-based technique are concentrated to the bottom-left, and the code is forced to arrive at sensors 5 and 6 at the middle and the top left of the beam, respectively. We also note that there are instances where the sampling-based method converges faster than the other two approaches owing to the randomness in the prediction of Bayes risk by its very inherent nature. However, we note a commonality in the prediction by all three approaches. All the significant additional sensor locations (the first six additional sensors) are spread across the vertical direction near the left boundary of the beam, which is suitable for the spring detection problem.

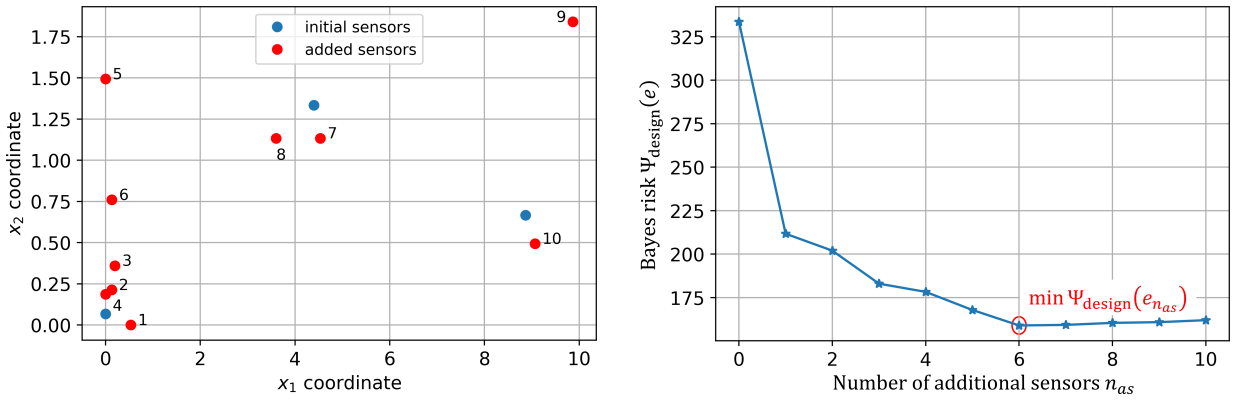

(a) Optimized sensor locations

(b) Bayes risk

Figure 13: Optimized sensor placement and the associated Bayes risk obtained using sampling-based method (approach 1)

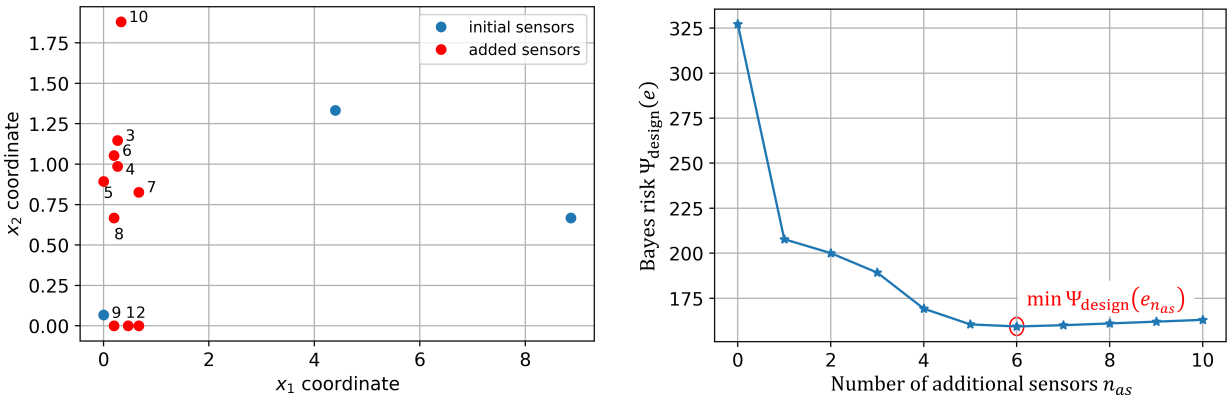

(a) Optimized sensor locations

(b) Bayes risk

Figure 14: Optimized sensor placement and the associated Bayes risk obtained using mean value approximation (approach 2)

5.2.3 Comparison of a Bayesian optimized sensor placement design with different initial designs

In this section, we compare the optimal sensor placement design evaluated using approach 3 for different initial designs e_0. Fig. 10 shows the sensor designs obtained when the initial sensor locations consist of well spread out strain-gauges across the beam. To demonstrate the effect of the choice of initial sensor designs, we consider three extreme cases of e_0 with the sensors concentrated on the bottom-left, bottom-right, and top-right, as shown in figure 15, 16, and 17.

The *Expected Improvement* function defined in Eq. (32) guides the optimization algorithm to *exploit* and *explore* the design space to pick for the next sample. The algorithm *exploits* the strain locations at which the GP mean function is larger, and it *explores* the strain locations where the GP standard deviation is larger. For instance, in Fig. 15, the algorithm obtains the first 4 additional sensors by exploiting the strain locations with higher GP mean value, whereas in Fig. 16, with e_0 consisting of concentrated bottom-right sensors, the algorithm obtains the additional sensors mostly by *exploring* the region of high GP standard-deviation. Since it evaluates the additional sensors 2, 3, 4, and 5 concentrated at the top left, it is forced to obtain sensors 6, 7, and 8 in the middle of the left end, leading to late convergence. Like the previous section, we do observe that irrespective of the initial design, the algorithm arrives at a sensor design that consists of additional sensor locations spread out across the left end.

We note that the beam is so finely meshed that there exists a correlation between the strain values. Therefore, there are non-unique sensor locations that are sampled by the acquisition function, leading to non-unique sensor design depending on different initial design e_0.

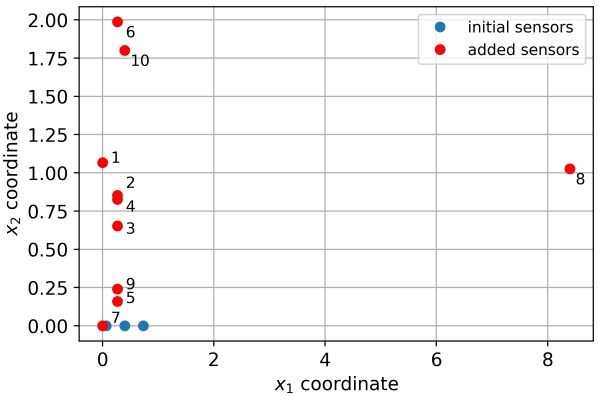

(a) Optimized sensor locations

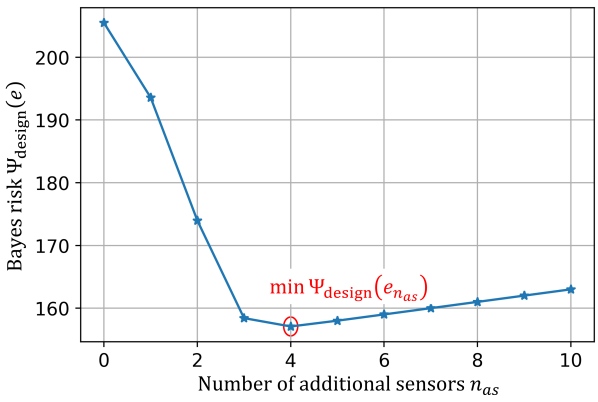

(b) Bayes risk

Figure 15: Optimized sensor placement and the associated Bayes risk obtained considering initial sensor design with three sensors concentrated at the bottom-left

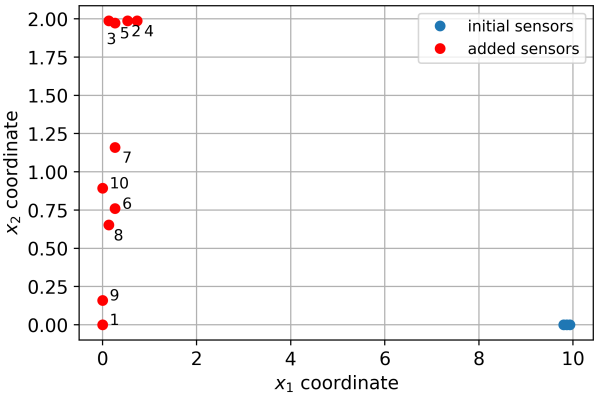

(a) Optimized sensor locations

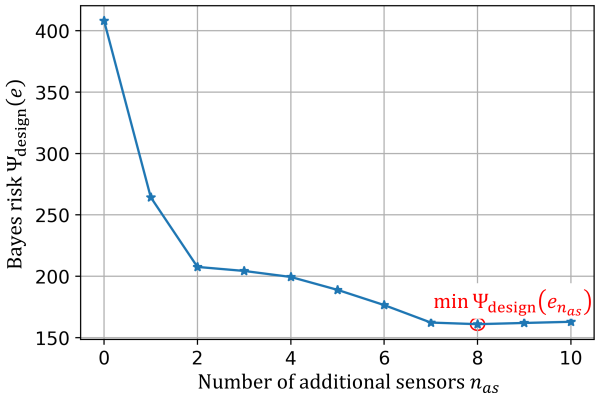

(b) Bayes risk

Figure 16: Optimized sensor placement and the associated Bayes risk obtained considering initial sensor design with three sensors concentrated at the bottom-right

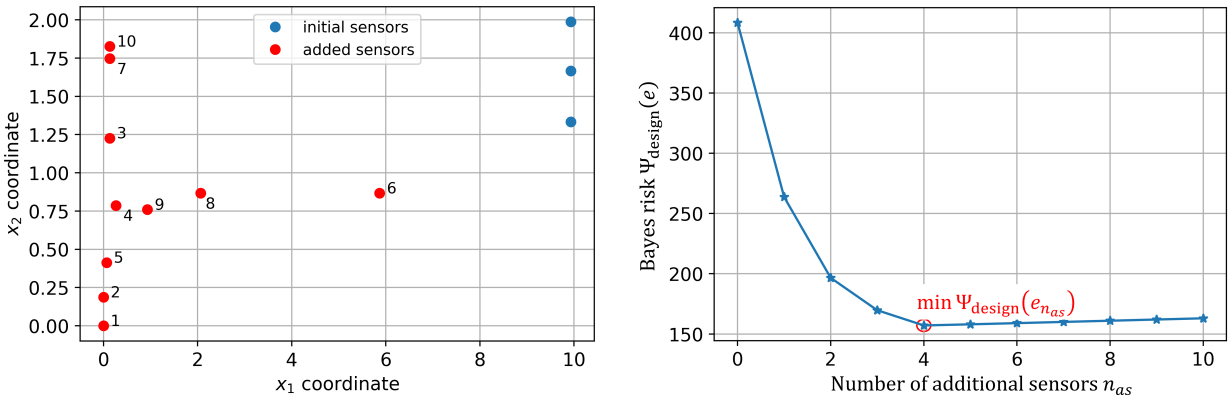

(a) Optimized sensor locations

(b) Bayes risk

Figure 17: Optimized sensor placement and the associated Bayes risk obtained considering initial sensor design with three sensors concentrated at the top-right

5.2.4 Comparison of a Bayesian optimized sensor placement design for different noise level in sensors

In this section, we compare the optimal sensor placement design evaluated using approach 3 and considering initial design e_0 with $N_0 = 3$ for different noise levels as depicted in Table 4. Case 1 to 4 represents various noise levels (standard deviation in the strain measurements) in ascending order. It is observed that the number of sensors in the optimal sensor design increases with the increase in noise level in the acquired data. This is an expected result since a large amount of data is required to compensate for the increased uncertainty due to higher noise levels.

Cases	Noise standard deviation σ_ϵ	Figure representing the resulting design	Number of sensors in optimal design
Case 1	5.0×10^{-7}	Fig. 18	4
Case 2	1.0×10^{-6}	Fig. 19	5
Case 3	2.5×10^{-6}	Fig. 20	9
Case 4	5.0×10^{-6}	Fig. 21	10

Table 4: Different cases of the noise level in strain gauges

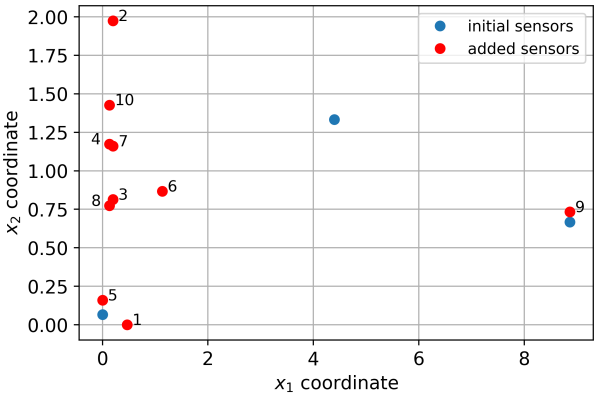

(a) Optimized sensor locations

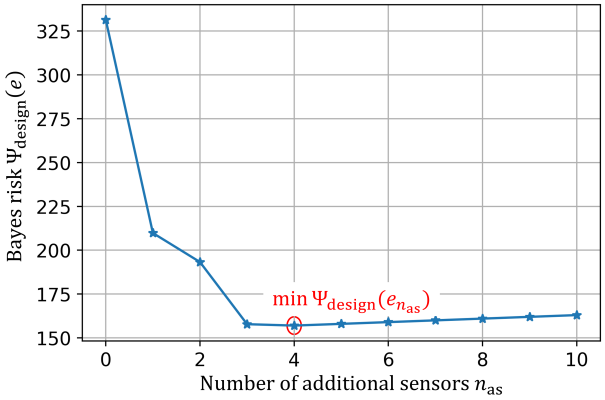

(b) Bayes risk

Figure 18: Optimized sensor placement and the associated Bayes risk obtained for case 1 of noise level

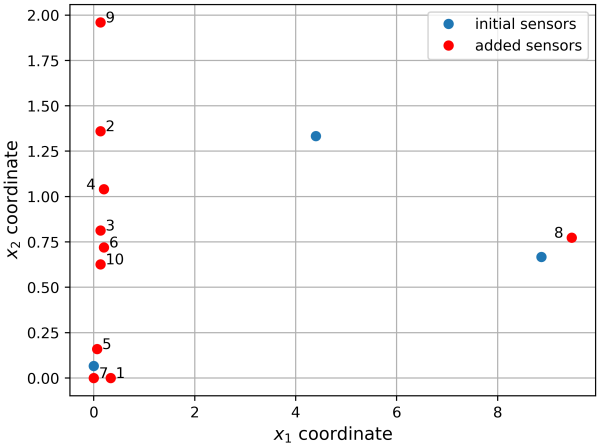

(a) Optimized sensor locations

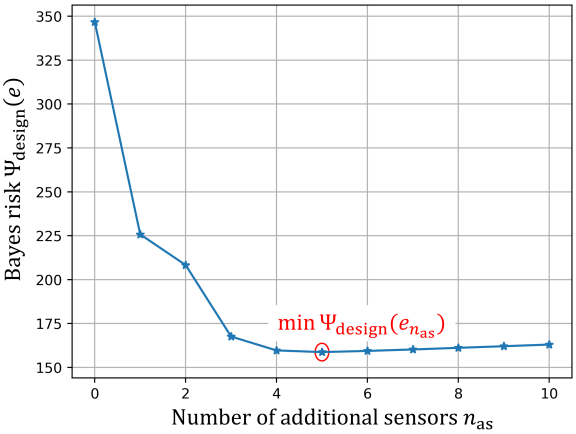

(b) Bayes risk

Figure 19: Optimized sensor placement and the associated Bayes risk obtained for case 2 of noise level

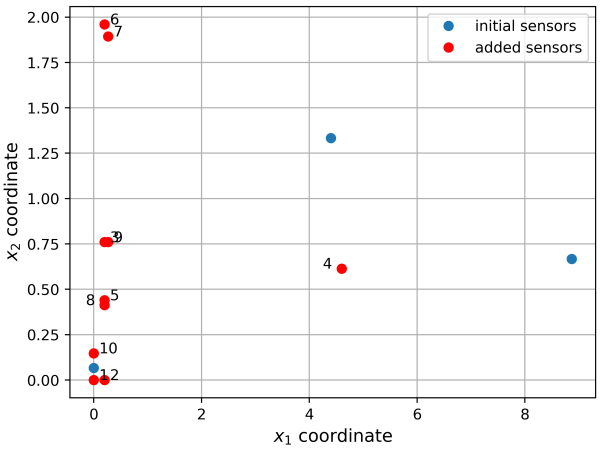

(a) Optimized sensor locations

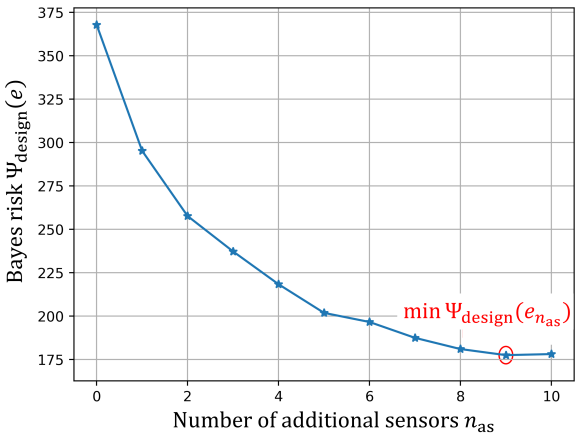

(b) Bayes risk

Figure 20: Optimized sensor placement and the associated Bayes risk obtained for case 3 of noise level

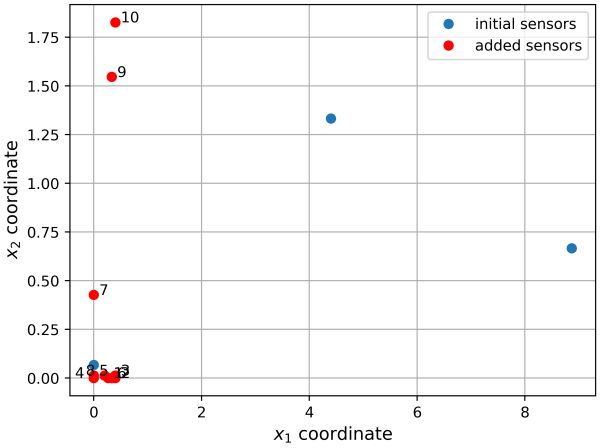

(a) Optimized sensor locations

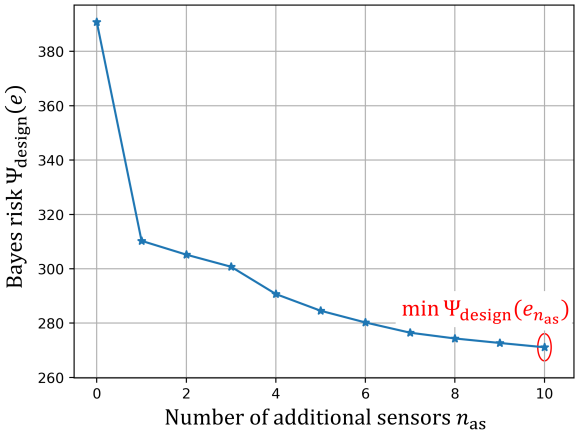

(b) Bayes risk

Figure 21: Optimized sensor placement and the associated Bayes risk obtained for case 4 of noise level

6 Summary and Conclusions

This paper details an optimal sensor design framework for structural health monitoring applications where detection of a critical state is of prime importance. The primary contribution of the paper is to present a sensor optimization framework and an algorithm that obtains the optimal sensor design yielding the least regrettable decision/inference of the state detection. The optimality criterion or the objective function used for optimization is the expected loss (arising as a consequence of decision making), the term also referred to as the *Bayes risk*. It is advantageous to use Bayes risk as it helps us incorporate the consequence-cost/regret of making a decision (extrinsic cost), as well as the intrinsic costs (e.g., sensor costs and their maintenance costs). A Bayes risk (or the expected loss/risk) minimized design leads to a prediction of the state that minimizes losses in an average sense.

The proposed optimal sensor placement design framework presented in this paper can be summarized in four sequential steps as illustrated in Fig. 1. The optimization framework proposed in this paper is demonstrated on an example problem, where the existence of the boundary springs is in question (a binary decision problem). Noteworthy conclusions are: (1) Bayesian optimized sensor design is better than the random design since it leads to less expected loss/regret as a consequence of making a decision all the while using less number of sensors; (2) Generally, the Bayes risk functional has a non-linear integrand and is a high dimensional integral that demands sophisticated numerical approaches to evaluate it. Among the three approaches investigated, approach 3 (using univariate dimensional reduction with Gauss-Hermite quadrature) is the most desirable; (3) Irrespective of the initial sensor design, the proposed optimization algorithm arrives at a sensor design that is suitable for desirable decision making. In the proposed example problem, irrespective of the initial design, the optimal design consisted of additional sensor locations spread out across the left end close to the springs; (4) It is observed that the number of sensors in the optimal sensor design increases with the increase in noise level in the acquired data.

Acknowledgment: Funding for this work was provided by the United States Army Corps of Engineers through the U.S. Army Engineer Research and Development Center Research Cooperative Agreement W912HZ-17-2-0024. We thank our colleague Professor Joel P. Conte in Department of Structural Engineering at UC San Diego for providing us with valuable advice and comments.

References

[1] C. R. Farrar and K. Worden, *Structural Health Monitoring: A Machine Learning Perspective*. Wiley, 2012.

[2] C. Farrar, G. Park, K. Farinholt, and M. Todd, "Integrated solutions to shm problems: an overview of shm research at the lanl/ucsd engineering institute," tech. rep., Los Alamos National Lab.(LANL), Los Alamos, NM (United States), 2010.

[3] R. A. Daniel, "Miter gates in some recent lock projects in the netherlands (stemmtore in einigen neuen schleusenanlagen in den niederlanden)," *Stahlbau*, vol. 69, no. 12, pp. 952–964, 2000.

[4] G. C. Richardson, "Navigation locks: navigation lock gates and valves," *Journal of the Waterways and Harbors Division*, vol. 90, no. 1, pp. 79–102, 1964.

[5] M. Parno, D. O'Connor, and M. Smith, "High dimensional inference for the structural health monitoring of lock gates," *arXiv preprint arXiv:1812.05529*, 2018.

[6] J. P. Schwieterman, S. Field, L. Fischer, and A. Pizzano, "An analysis of the economic effects of terminating operations at the chicago river controlling works and o'brien locks on the chicago area waterway system," *DePaul University, Chicago, IL*, 2010.

[7] Y. Yang, R. Madarshahian, and M. D. Todd, "Bayesian damage identification using strain data from lock gates," in *Dynamics of Civil Structures, Volume 2*, pp. 47–54, Springer, 2020.

[8] S. D. Foltz, "Investigation of mechanical breakdowns leading to lock closures," tech. rep., ERDC-CERL CHAMPAIGN United States, 2017.

[9] B. A. Eick, Z. R. Treece, B. F. Spencer Jr, M. D. Smith, S. C. Sweeney, Q. G. Alexander, and S. D. Foltz, "Automated damage detection in miter gates of navigation locks," *Structural Control and Health Monitoring*, vol. 25, no. 1, p. e2053, 2018.

[10] E. Wilkins, "Cumulative damage in fatigue," in *Colloquium on Fatigue/Colloque de Fatigue/Kolloquium über Ermüdungsfestigkeit*, pp. 321–332, Springer, 1956.

[11] M. A. Vega and M. D. Todd, "A variational bayesian neural network for structural health monitoring and cost-informed decision-making in miter gates," *Structural Health Monitoring*, p. 1475921720904543, 2020.

[12] S. Thöns and M. H. Faber, "Assessing the value of structural health monitoring," *ICOSSAR'13 - 11th International conference on structural safety and reliability - Safety, reliability, risk and life-cycle performance of structures and infrastructures (Proceedings)*, 2013.

[13] P. Nath, Z. Hu, and S. Mahadevan, "Sensor placement for calibration of spatially varying model parameters," *Journal of Computational Physics*, vol. 343, pp. 150–169, 2017.

[14] S. L. Padula and R. K. Kincaid, "Optimization strategies for sensor and actuator placement," *NASA/TM-1999-209126*, 1999.

[15] C. Malings and M. Pozzi, "Optimal sensor placement and scheduling with value of information for spatio-temporal infrastructure system management," in *Proc., 12th Int. Conf. on Structural Safety and Reliability*, pp. 3320–3330, 2017.

[16] E. Chan, "Optimal design of building structures using genetic algorithms," *California Institute of Technology*, Report No. EERL 97-06, 1997.

[17] T.-H. Yi, H.-N. Li, and M. Gu, "A new method for optimal selection of sensor location on a high-rise building using simplified finite element model," *Structural Engineering and Mechanics*, vol. 37, no. 6, pp. 671–684, 2011.

[18] S. R. Peddada, P. J. Tannous, A. G. Alleyne, and J. T. Allison, "Optimal sensor placement methods in active high power density electronic systems with experimental validation," *Journal of Mechanical Design*, vol. 142, no. 2, 2020.

[19] V. Akbarzadeh, J.-C. Lévesque, C. Gagné, and M. Parizeau, "Efficient sensor placement optimization using gradient descent and probabilistic coverage," *Sensors*, vol. 14, no. 8, pp. 15525–15552, 2014.

[20] E. Peh and Y.-C. Liang, "Optimization for cooperative sensing in cognitive radio networks," in *2007 IEEE Wireless Communications and Networking Conference*, pp. 27–32, IEEE, 2007.

[21] W. A. Maul, G. Kopasakis, L. M. Santi, T. S. Sowers, and A. Chicatelli, "Sensor selection and optimization for health assessment of aerospace systems," *Journal of Aerospace Computing, Information, and Communication*, vol. 5, no. 1, pp. 16–34, 2008.

[22] C. Papadimitriou, J. L. Beck, and S.-K. Au, "Entropy-based optimal sensor location for structural model updating," *Journal of Vibration and Control*, vol. 6, no. 5, pp. 781–800, 2000.

[23] F. Unwadia, "Methodology for optimal sensor locations for parameter identification in dynamic system," *Journal of Engineering Mechanics*, vol. 120, pp. 368–390, 1994.

[24] M. Basseville, A. Benveniste, G. Moustakides, and A. Rougee, "Optimal sensor location for detecting changes in dynamical behavior," *IEEE Transactions on Automatic control*, vol. 32, no. 12, pp. 1067–1075, 1987.

[25] E. B. Flynn and M. D. Todd, "A bayesian approach to optimal sensor placement for structural health monitoring with application to active sensing," *Mechanical Systems and Signal Processing*, vol. 24, no. 4, pp. 891–903, 2010.

[26] M. D. Todd and E. B. Flynn, "A bayesian experimental design approach for structural health monitoring," in *Proceedings of the XIV International Symposium on Dynamic Problems of Mechanics (DINAME 2011), Brazil*, 2011.

[27] F. Chaloner and I. Verdinelli, "Bayesian experimental design: A review," *Statistical Science*, vol. 10, no. 3, pp. 273–304, 1995.

[28] L. Bottou, "Large-scale machine learning with stochastic gradient descent," in *Proceedings of COMPSTAT'2010*, pp. 177–186, Springer, 2010.

[29] S. S. Ram, A. Nedic, and V. V. Veeravalli, "Stochastic incremental gradient descent for estimation in sensor networks," in *2007 Conference Record of the Forty-First Asilomar Conference on Signals, Systems and Computers*, pp. 582–586, IEEE, 2007.

[30] P. K. Agarwal, E. Ezra, and S. K. Ganjugunte, "Efficient sensor placement for surveillance problems," in *International Conference on Distributed Computing in Sensor Systems*, pp. 301–314, Springer, 2009.

[31] S. Jin, M. Zhou, and A. S. Wu, "Sensor network optimization using a genetic algorithm," in *Proceedings of the 7th world multiconference on systemics, cybernetics and informatics*, pp. 109–116, 2003.

[32] T.-H. Yi, H.-N. Li, and M. Gu, "Optimal sensor placement for health monitoring of high-rise structure based on genetic algorithm," *Mathematical Problems in Engineering*, vol. 2011, 2011.

[33] D. R. Jones, M. Schonlau, and W. J. Welch, "Efficient global optimization of expensive black-box functions," *Journal of Global optimization*, vol. 13, no. 4, pp. 455–492, 1998.

[34] Z. Hu, S. Nannapaneni, and S. Mahadevan, "Efficient kriging surrogate modeling approach for system reliability analysis," *AI EDAM*, vol. 31, no. 2, pp. 143–160, 2017.

[35] P. I. Frazier, "A tutorial on bayesian optimization," *arXiv preprint arXiv:1807.02811*, 2018.

[36] J. Mockus, V. Tiesis, and A. Zilinskas, "The application of bayesian methods for seeking the extremum," *Towards Global Optimization*, vol. 2, no. 2, pp. 117–129, 1978.

[37] D. R. Jones, M. Schonlau, and W. J. Welch, "Efficient global optimization of expensive black-box functions," *Journal of Global Optimization*, vol. 13, no. 4, pp. 455–492, 1998.

[38] F. McKenna, "Opensees: a framework for earthquake engineering simulation," *Computing in Science & Engineering*, vol. 13, no. 4, pp. 58–66, 2011.

[39] M. Chadha and M. D. Todd, "A comprehensive kinematic model of single-manifold cosserat beam structures with application to a finite strain measurement model for strain gauges," *International Journal of Solids and Structures*, vol. 159, pp. 58–76, 2019.

[40] M. D. McKay, R. J. Beckman, and W. J. Conover, "A comparison of three methods for selecting values of input variables in the analysis of output from a computer code," *Technometrics*, vol. 42, no. 1, pp. 55–61, 2000.

[41] M. Ramancha, R. Astroza, J. P. Conte, J. I. Restrepo, and M. D. Todd, "Bayesian nonlinear finite element model updating of a full-scale bridge-column using sequential monte carlo," in *Proceedings of the 38th IMAC, A Conference and Exposition on Structural Dynamics 2020*, Springer, 2021.

[42] M. Moustapha, J.-M. Bourinet, B. Guillaume, and B. Sudret, "Comparative study of kriging and support vector regression for structural engineering applications," *ASCE-ASME Journal of Risk and Uncertainty in Engineering Systems, Part A: Civil Engineering*, vol. 4, no. 2, p. 04018005, 2018.

[43] L. Yu, S. Wang, and K. K. Lai, "A neural-network-based nonlinear metamodeling approach to financial time series forecasting," *Applied Soft Computing*, vol. 9, no. 2, pp. 563–574, 2009.

[44] G. Capellari, E. Chatzi, and S. Mariani, "Cost–benefit optimization of structural health monitoring sensor networks," *Sensors*, vol. 18, no. 7, p. 2174, 2018.

[45] S. Rahman and H. Xu, "A univariate dimension-reduction method for multi-dimensional integration in stochastic mechanics," *Probabilistic Engineering Mechanics*, vol. 19, no. 4, pp. 393–408, 2004.

[46] Y. Yang, M. Chadha, Z. Hu, M. A. Vega, M. D. Parno, and M. D. Todd, "A probabilistic optimal sensor design approach for structural health monitoring using risk-weighted f-divergence," *Mechanical Systems and Signal Processing*, vol. 161, p. 107920, 2021.

[47] M. Chadha, Z. Hu, and M. D. Todd, "An alternative quantification of the value of information in structural health monitoring," *Structural Health Monitoring*, p. 14759217211028439, 2021.